

Outlier Detection Using Distributionally Robust Optimization under the Wasserstein Metric

Ruidi Chen,^{*} and Ioannis Ch. Paschalidis,[†]

February 10, 2022

Abstract

We present a *Distributionally Robust Optimization (DRO)* approach to outlier detection in a linear regression setting, where the closeness of probability distributions is measured using the Wasserstein metric. Training samples contaminated with outliers skew the regression plane computed by least squares and thus impede outlier detection. Classical approaches, such as robust regression, remedy this problem by downweighting the contribution of atypical data points. In contrast, our Wasserstein DRO approach hedges against a family of distributions that are close to the empirical distribution. We show that the resulting formulation encompasses a class of models, which include the regularized *Least Absolute Deviation (LAD)* as a special case. We provide new insights into the regularization term and give guidance on the selection of the regularization coefficient from the standpoint of a confidence region. We establish two types of performance guarantees for the solution to our formulation under mild conditions. One is related to its out-of-sample behavior, and the other concerns the discrepancy between the estimated and true regression planes. Extensive numerical results demonstrate the superiority of our approach to both robust regression and the regularized LAD in terms of estimation accuracy and outlier detection rates.

1 Introduction

Outlier detection is an integral part of data mining and has found extensive use in diverse fields such as fraud detection, cyber security, and medical informatics. An outlier is an observation that deviates markedly from others in the available sample and arises often due to systematic changes or human error.

^{*}† R. Chen is with the Division of Systems Engineering, Boston University, Boston, MA 02215, USA. E-mail: rchen15@bu.edu

[†]‡ I. Ch. Paschalidis is with the Department of Electrical and Computer Engineering, the Division of Systems Engineering, and the Department of Biomedical Engineering, Boston University, Boston, MA 02215, USA. E-mail: yannisp@bu.edu, URL: <http://sites.bu.edu/paschalidis/>.

The identification of outliers is important in two aspects. On one hand, in cases where outliers are erroneous data points, it helps to delete the aberrant observations and enables purification of the dataset. On the other hand, abnormal data might contain useful information which could help to identify systematic errors and improve system performance. Our interest in outlier detection comes from its application in CT radiation overdose detection. There has been a growing concern about excessive exposure to CT radiation in recent years, which is known to lead to increased cancer risk. Detecting CT scans which led to a higher radiation dose than medically necessary, and identifying the potential reasons, can help guide effective interventions [see Raff et al., 2009, Siegelman and Gress, 2013, Boone et al., 2012].

Classical outlier detection techniques can be categorized into direct and indirect methods, as defined by Hadi and Simonoff [1993]. The direct methods implement algorithms to sequentially remove outliers or add clean observations based on some criterion, see Hadi and Simonoff [1993], Sebert et al. [1998], Swallow and Kianifard [1996]. By contrast, the indirect procedures identify outliers based on the residuals from robust regression estimates. The reason for relying on robust estimators rather than *Ordinary Least Squares (OLS)*, lies in the non-typicality of the samples which are contaminated with outliers. Instead of assigning the same weight to every sample as in OLS, robust regression downweights the aberrant observations and is thus less vulnerable to outliers. The most commonly used robust regression techniques, including *M*-estimation [Huber, 1964, 1973], *Least Median of Squares (LMS)* [Rousseeuw, 1984], *Least Trimmed Squares (LTS)* [Rousseeuw, 1985], *S*-estimation [Rousseeuw and Yohai, 1984], and *MM*-estimation [Yohai, 1987], are elaborated in the book of Rousseeuw and Leroy [2005]. *M*-estimation is the simplest approach both computationally and theoretically but cannot handle data which are contaminated in the covariate space, in which case high breakdown value methods such as *LTS*, *LMS*, and *S*-estimation are needed. *MM*-estimation is a combination of *M*-estimation and the high breakdown value method.

Different from traditional robust estimators, another way of coping with unreliable, contaminated samples is to hedge against a family of distributions that are of interest. We essentially want to infer the true data-generating mechanism and detect samples that violate it. This reduces to minimizing some expected loss under a reasonable probability distribution \mathbb{P} , which falls into the field of stochastic optimization [Shapiro et al., 2014]. The distribution function \mathbb{P} is not directly observable and must be inferred from samples. However, using just a single distribution that works well for observed samples does not necessarily result in satisfactory out-of-sample performance. *Distributionally Robust Optimization (DRO)* solves this problem through minimizing the worst-case loss over a probabilistic ambiguity set \mathcal{P} characterized by certain known properties of the true data-generating distribution. For example, Mehrotra and Zhang [2014] study the distributionally robust least squares problem with \mathcal{P} defined through (1) moment constraints, (2) norm bounds with moment constraints, (3) or a confidence region over a reference probability measure. There is also some work focusing on deterministic robustness. El Ghaoui and Lebret [1997]

consider the least squares problem with unknown but bounded, non-random disturbance and solve it in polynomial time. Xu et al. [2010] study the robust linear regression problem with norm-bounded feature perturbation and show that it is equivalent to the ℓ_1 -regularized regression.

The existing literature on DRO can be split into two main branches according to the way in which \mathcal{P} is defined. One is through a moment ambiguity set, which contains all distributions that satisfy certain moment constraints [see Popescu, 2007, Delage and Ye, 2010, Goh and Sim, 2010, Zymler et al., 2013, Wiesemann et al., 2014]. In many cases it leads to a tractable DRO problem but has been criticized for yielding overly conservative solutions [Wang et al., 2016]. The other is to define \mathcal{P} as a ball of distributions using some probability distance functions such as the ϕ -divergences [Bayraktar and Love, 2015], which include the Kullback-Leibler (KL) divergence [Hu and Hong, 2013, Jiang and Guan, 2015] as a special case, the Prokhorov metric [Erdoğan and Iyengar, 2006], and the Wasserstein distance [Esfahani and Kuhn, 2015, Gao and Kleywegt, 2016, Zhao and Guan, 2015].

In this paper we consider a DRO problem with \mathcal{P} containing distributions that are close to the discrete empirical distribution in the sense of Wasserstein distance. The reason for choosing the Wasserstein metric is two-fold. On one hand, the Wasserstein ambiguity set is rich enough to contain both continuous and discrete relevant distributions, while other metrics such as the KL divergence, exclude all continuous distributions if the nominal distribution is discrete [Esfahani and Kuhn, 2015, Gao and Kleywegt, 2016]. Furthermore, considering distributions within a KL distance from the empirical, does not allow for probability mass outside the support of the empirical distribution. On the other hand, the measure concentration results guarantee that the Wasserstein set contains the true data-generating distribution with high confidence for a sufficiently large sample size [Fournier and Guillin, 2015]. The image retrieval example in Gao and Kleywegt [2016] suggests that the pathological distribution is closer to the observed histogram than the true distribution in the sense of KL divergence, whereas the Wasserstein distance does not exhibit such a problem. The reason lies in that ϕ -divergence does not incorporate a notion of closeness between two points, which in the context of image retrieval represents the perceptual similarity in color.

Our Wasserstein DRO formulation essentially incorporates a class of models whose specific form depends on the norm space that the Wasserstein metric is defined on. For properly selected norm spaces, our formulation reduces to the regularized *Least Absolute Deviation (LAD)* [Pollard, 1991, Wang et al., 2006], which has been well studied in the literature. However, we want to emphasize the following important differences between them. In earlier LAD work, ℓ_1/ℓ_2 regularization is used to prevent overfitting, or to recover a sparse coefficient vector and reduce the prediction error, as well as the variance of the estimated coefficients when predictors are highly correlated. In our work, the regularization term controls the conservativeness of the Wasserstein set. Instead of viewing it as an arbitrary regularizer, it is more appropriate to interpret it as a control over the amount of ambiguity in the data. Our regularization coefficient

is the radius of the Wasserstein ball. This connection suggests how to set it and is not present in the regularized LAD literature.

The connection between robustness and regularization has been studied in several different settings. For example, in classification problems, Xu et al. [2009] show the equivalence between the regularized support vector machines (SVMs) and a robust optimization formulation, by allowing potentially correlated disturbances in the covariates. Shafieezadeh-Abadeh et al. [2015] consider a robust version of logistic regression under the assumption that the probability distributions under consideration lie in a Wasserstein ball, and they show that the regularized logistic regression is a special case of this robust formulation. The equivalence between robustness and regularization has also been established in Bishop [1995], El Ghaoui and Le Bret [1997], Xu et al. [2010]. Our work explores the generalization ability of the regularization term in the context of LAD which provides a loss function that is less sensitive to outliers. The superiority of our formulation could be attributed to both the selection of the LAD loss, and the robustness explanation of the regularization term.

We summarize our contributions as follows:

1. We develop a DRO approach to robustify linear regression using an ℓ_1 loss function and an ambiguity set around the empirical distribution of the training samples defined based on the Wasserstein metric. The formulation is general enough to include any norm-induced Wasserstein metric and incorporate additional regularization constraints on the regression coefficients (e.g., ℓ_1 -norm constraints). It provides an intuitive connection between the amount of ambiguity allowed and a regularization penalty term in the robust formulation, which provides a natural way to adjust the latter.
2. Our approach leads to tractable optimization problems for computing the robust regression coefficients. For example, using the Wasserstein metric induced by the ℓ_2 -norm and under additional linear or convex quadratic constraints on the regression coefficients, the robust formulation is a convex quadratic programming problem. As another example, using the Wasserstein metric induced by the ℓ_1 -norm and under additional linear constraints on the regression coefficients, the robust formulation is a linear programming problem.
3. We establish out-of-sample performance guarantees both on the value of the loss function and the discrepancy between the estimated and the true regression coefficients. Our guarantees are novel in the robust regression setting and different from earlier work in the DRO literature.
4. We focus our work on the problem of outlier detection based on linear regression residuals and show that our approach outperforms earlier robust regression and regularized LAD formulations under a variety of scenarios for generating outliers.

The rest of the paper is organized as follows. In Section 2, we introduce the Wasserstein metric and derive the general Wasserstein DRO formulation in a linear regression framework. Section 3 establishes performance guarantees for both the general formulation and the special case where the Wasserstein metric is defined on the ℓ_1 -norm space. The numerical experimental results are presented in Section 4. We conclude the paper in Section 5.

Notational conventions: We use boldfaced lowercase letters to denote vectors, ordinary lowercase letters to denote scalars, boldfaced uppercase letters to denote matrices, and calligraphic capital letters to denote sets. \mathbb{E} denotes expectation and \mathbb{P} probability of an event. All vectors are column vectors. For space saving reasons, we write $\mathbf{x} = (x_1, \dots, x_{\dim(\mathbf{x})})$ to denote the column vector \mathbf{x} , where $\dim(\mathbf{x})$ is the dimension of \mathbf{x} . We use prime to denote the transpose of a vector, $\|\cdot\|$ for the general norm operator, $\|\cdot\|_2$ for the ℓ_2 norm, $\|\cdot\|_1$ for the ℓ_1 norm, and $\|\cdot\|_\infty$ for the infinity norm. $\mathcal{P}(\mathcal{Z})$ denotes the set of probability measures supported on \mathcal{Z} . \mathbf{e}_i denotes the i -th unit vector, $\mathbf{0}$ a vector of zeroes, and \mathbf{I} the identity matrix.

2 Problem Formulation

In this section we introduce the Wasserstein metric and derive our Wasserstein DRO formulation in a linear regression framework. As a key ingredient of our approach, the Wasserstein metric measures the distance in the space of probability distributions in terms of the integrals of stochastic functions under distributions of interest. Different from some popular statistical metrics, such as the KL divergence [Jiang and Guan, 2015] and Total Variation distance [Kennedy et al., 1989, Sun and Xu, 2015], the Wasserstein metric incorporates a notion of cost that evaluates the closeness between points, which makes it a more reasonable and competitive choice in many real applications. We have already discussed the advantages of the Wasserstein metric in Section 1.

2.1 Wasserstein Metric

Let (\mathcal{Z}, s) be a metric space where \mathcal{Z} is a set and s is a metric on \mathcal{Z} . The Wasserstein metric of order p defines the distance between two probability distributions \mathbb{Q}_1 and \mathbb{Q}_2 in the following way:

$$W_p(\mathbb{Q}_1, \mathbb{Q}_2) \triangleq \left(\min_{\Pi \in \mathcal{P}(\mathcal{Z} \times \mathcal{Z})} \left\{ \int_{\mathcal{Z} \times \mathcal{Z}} (s(\mathbf{z}_1, \mathbf{z}_2))^p \Pi(d\mathbf{z}_1, d\mathbf{z}_2) \right\} \right)^{1/p}, \quad (1)$$

where Π is the joint distribution of \mathbf{z}_1 and \mathbf{z}_2 with marginals \mathbb{Q}_1 and \mathbb{Q}_2 , respectively. The Wasserstein distance between \mathbb{Q}_1 and \mathbb{Q}_2 represents the cost of an optimal mass transportation plan, where the cost is measured through the metric s . A dual representation for (1), due to Kantorovich's duality, is found

to be convenient and useful in some DRO problems:

$$\left(W_p(\mathbb{Q}_1, \mathbb{Q}_2)\right)^p = \sup_{f \in L^1(\mathbb{Q}_1), g \in L^1(\mathbb{Q}_2)} \left\{ \int_{\mathcal{Z}} f(\mathbf{z}_1) \mathbb{Q}_1(d\mathbf{z}_1) + \int_{\mathcal{Z}} g(\mathbf{z}_2) \mathbb{Q}_2(d\mathbf{z}_2) : \right. \\ \left. f(\mathbf{z}_1) + g(\mathbf{z}_2) \leq (s(\mathbf{z}_1, \mathbf{z}_2))^p, \forall \mathbf{z}_1, \mathbf{z}_2 \in \mathcal{Z} \right\}, \quad (2)$$

where $L^1(\mathbb{Q})$ denotes the L^1 space of \mathbb{Q} -measurable functions. When $p = 1$, by the Kantorovich-Rubinstein Theorem [Kantorovich and Rubinstein, 1958], (2) can be simplified to:

$$W_1(\mathbb{Q}_1, \mathbb{Q}_2) = \sup_{f \in \mathcal{L}} \left\{ \int_{\mathcal{Z}} f(\mathbf{z}) \mathbb{Q}_1(d\mathbf{z}) - \int_{\mathcal{Z}} f(\mathbf{z}) \mathbb{Q}_2(d\mathbf{z}) \right\}, \quad (3)$$

with \mathcal{L} being the space of all Lipschitz continuous functions satisfying $|f(\mathbf{z}_1) - f(\mathbf{z}_2)| \leq s(\mathbf{z}_1, \mathbf{z}_2)$, $\forall \mathbf{z}_1, \mathbf{z}_2 \in \mathcal{Z}$.

In this paper, we consider the metric s induced by some norm $\|\cdot\|$ and order $p = 1$. Allowing a higher order Wasserstein distance might give more flexibility in building the ambiguity set and controlling the conservativeness of the DRO approach. However, as we demonstrate in Section 2.2, $p = 1$ ensures the finite growth rate of our adopted loss function as the uncertainty parameter approaches infinity. Strong duality fails to hold when the growth rate of the loss function is unbounded, in which case the DRO problem becomes intractable.

2.2 Wasserstein DRO Formulation for Outlier Detection

Before formulating the DRO problem for outlier detection, we first introduce some definitions that will be used in later development.

Definition 1 (Dual norm) *Given a norm $\|\cdot\|$ on \mathbb{R}^m , the dual norm $\|\cdot\|_*$ is defined as:*

$$\|\boldsymbol{\theta}\|_* \triangleq \sup_{\|\mathbf{z}\| \leq 1} \boldsymbol{\theta}'\mathbf{z}. \quad (4)$$

It can be shown from (4) that for any vectors $\boldsymbol{\theta}, \mathbf{z}$, given a norm $\|\cdot\|$, the following Cauchy-Schwarz inequality holds:

$$|\boldsymbol{\theta}'\mathbf{z}| \leq \|\boldsymbol{\theta}\|_* \|\mathbf{z}\|. \quad (5)$$

Definition 2 (Conjugate function) *For a function $h(\mathbf{z})$, its conjugate $h^*(\cdot)$ is defined as:*

$$h^*(\boldsymbol{\theta}) \triangleq \sup_{\mathbf{z} \in \text{dom } h} \{\boldsymbol{\theta}'\mathbf{z} - h(\mathbf{z})\}, \quad (6)$$

where $\text{dom } h$ denotes the domain of the function h .

Now let us discuss the outlier detection problem. Suppose we have N independently and identically distributed samples $(\mathbf{x}_1, y_1), \dots, (\mathbf{x}_N, y_N)$, where y_i is the i th response variable and \mathbf{x}_i is an $(m - 1)$ -dimensional vector of features. (We set the first element of \mathbf{x}_i to 1 to include the intercept as part of the features.) Each sample is drawn with probability q from the outlying distribution \mathbb{P}_{out} and with probability $1 - q$ from the true distribution \mathbb{P} (clean data). $\hat{\mathbb{P}}_N$ is the discrete uniform distribution over these N samples. Our goal is to first obtain an accurate estimate of the regression plane determined by the clean data and then detect outliers based on this estimate. Consider an ℓ_1 loss function in the linear regression setting. Using (\mathbf{x}, y) to denote the feature and response variables, our Wasserstein DRO problem is formulated as:

$$\inf_{\tilde{\boldsymbol{\beta}} \in \tilde{\mathcal{B}}} \sup_{\mathbb{Q} \in \Omega} \mathbb{E}^{\mathbb{Q}}[|y - \mathbf{x}'\tilde{\boldsymbol{\beta}}|] \triangleq \inf_{\boldsymbol{\beta} \in \mathcal{B}} \sup_{\mathbb{Q} \in \Omega} \mathbb{E}^{\mathbb{Q}}[|\mathbf{z}'\boldsymbol{\beta}|], \quad (7)$$

where $\tilde{\boldsymbol{\beta}}$ is the regression coefficient vector that belongs to some set $\tilde{\mathcal{B}}$; $\boldsymbol{\beta} \triangleq (-\tilde{\boldsymbol{\beta}}, 1)$; $\mathbf{z} \triangleq (\mathbf{x}, y)$; $\mathcal{B} = \{\boldsymbol{\beta} : \boldsymbol{\beta} = (-\tilde{\boldsymbol{\beta}}, 1), \tilde{\boldsymbol{\beta}} \in \tilde{\mathcal{B}}\}$. \mathcal{B} could be \mathbb{R}^m , or $\mathcal{B} = \{\boldsymbol{\beta} : \|\boldsymbol{\beta}\|_1 \leq l\}$ if we wish to induce sparsity, with l being some pre-specified number; \mathbb{Q} is the probability distribution of \mathbf{z} , belonging to some set Ω and defined as:

$$\Omega \triangleq \{\mathbb{Q} \in \mathcal{P}(\mathcal{Z}) : W_1(\mathbb{Q}, \hat{\mathbb{P}}_N) \leq \epsilon\},$$

where \mathcal{Z} is the set of possible values for \mathbf{z} ; $\mathcal{P}(\mathcal{Z})$ is the space of all probability distributions supported on \mathcal{Z} ; ϵ is a pre-specified radius of the Wasserstein ball; and $W_1(\mathbb{Q}, \hat{\mathbb{P}}_N)$ is the order-1 Wasserstein distance between \mathbb{Q} and $\hat{\mathbb{P}}_N$ defined as in (3) with the metric s being induced by some norm $\|\cdot\|$. The formulation in (7) is robust since it minimizes over the regression coefficients the worst case expected loss, that is, the expected loss maximized over all probability distributions in the ambiguity set Ω .

Defining the loss function $h_{\boldsymbol{\beta}}(\mathbf{z}) \triangleq |\mathbf{z}'\boldsymbol{\beta}|$, and using a fixed \mathbf{z}_0 , the growth rate of our loss function is:

$$\begin{aligned} \limsup_{\|\mathbf{z} - \mathbf{z}_0\| \rightarrow \infty} \frac{h_{\boldsymbol{\beta}}(\mathbf{z}) - h_{\boldsymbol{\beta}}(\mathbf{z}_0)}{\|\mathbf{z} - \mathbf{z}_0\|} &\leq \limsup_{\|\mathbf{z} - \mathbf{z}_0\| \rightarrow \infty} \frac{|\boldsymbol{\beta}'(\mathbf{z} - \mathbf{z}_0)|}{\|\mathbf{z} - \mathbf{z}_0\|} \\ &\leq \limsup_{\|\mathbf{z} - \mathbf{z}_0\| \rightarrow \infty} \frac{\|\mathbf{z} - \mathbf{z}_0\| \|\boldsymbol{\beta}\|_*}{\|\mathbf{z} - \mathbf{z}_0\|} \\ &= \|\boldsymbol{\beta}\|_*, \end{aligned} \quad (8)$$

where the last inequality used (5). Note that the growth rate does not depend on the choice of \mathbf{z}_0 [see Gao and Kleywegt, 2016, Lemma 4]. From (8) it is easily seen that the growth rate is finite as long as the dual norm of $\boldsymbol{\beta}$ is bounded. Therefore, the order-1 Wasserstein metric is sufficient to ensure the tractability of the DRO problem (7).

To convert (7) into a tractable optimization problem, we apply a key result in Esfahani and Kuhn [2015, Theorem 6.3] which states that when the set \mathcal{Z} is

closed and convex, for any $\epsilon \geq 0$,

$$\sup_{\mathbf{Q} \in \Omega} \mathbb{E}^{\mathbf{Q}}[|\mathbf{z}'\boldsymbol{\beta}|] \leq \kappa\epsilon + \frac{1}{N} \sum_{i=1}^N |\mathbf{z}'_i\boldsymbol{\beta}|, \quad (9)$$

where \mathbf{z}_i is the i th sample of \mathbf{z} ; and $\kappa = \sup\{\|\boldsymbol{\theta}\|_* : h_{\boldsymbol{\beta}}^*(\boldsymbol{\theta}) < \infty\}$. Note that κ is a function of $\boldsymbol{\beta}$. Through (9), we can relax problem (7) by minimizing the right hand side of (9) instead of the worst-case expected loss. Moreover, as shown in Esfahani and Kuhn [2015], (9) becomes an equality when $\mathcal{Z} = \mathbb{R}^m$. In Theorem 2.1, we compute the value of κ for the specific ℓ_1 loss function we use.

Theorem 2.1 *Define $\kappa = \sup\{\|\boldsymbol{\theta}\|_* : h_{\boldsymbol{\beta}}^*(\boldsymbol{\theta}) < \infty\}$, where $\|\cdot\|_*$ is the dual norm defined in (4), and $h_{\boldsymbol{\beta}}^*(\cdot)$ is the conjugate function of $h_{\boldsymbol{\beta}}(\cdot)$ as defined in (6). When the loss function is $h_{\boldsymbol{\beta}}(\mathbf{z}) = |\mathbf{z}'\boldsymbol{\beta}|$, we have $\kappa = \|\boldsymbol{\beta}\|_*$.*

Proof: First rewrite κ as:

$$\kappa = \sup\left\{\|\boldsymbol{\theta}\|_* : \sup_{\mathbf{z}|\mathbf{z}'\boldsymbol{\beta} \geq 0} \{(\boldsymbol{\theta} - \boldsymbol{\beta})'\mathbf{z}\} < \infty, \sup_{\mathbf{z}|\mathbf{z}'\boldsymbol{\beta} \leq 0} \{(\boldsymbol{\theta} + \boldsymbol{\beta})'\mathbf{z}\} < \infty\right\}.$$

Consider now the two linear optimization problems A and B:

$$\text{Problem A:} \quad \begin{array}{ll} \max & (\boldsymbol{\theta} - \boldsymbol{\beta})'\mathbf{z} \\ \text{s.t.} & \mathbf{z}'\boldsymbol{\beta} \geq 0. \end{array}$$

$$\text{Problem B:} \quad \begin{array}{ll} \max & (\boldsymbol{\theta} + \boldsymbol{\beta})'\mathbf{z} \\ \text{s.t.} & \mathbf{z}'\boldsymbol{\beta} \leq 0. \end{array}$$

Form the dual problems using dual variables r_A and r_B , respectively:

$$\text{Dual-A:} \quad \begin{array}{ll} \min & 0 \cdot r_A \\ \text{s.t.} & \boldsymbol{\beta}r_A = \boldsymbol{\theta} - \boldsymbol{\beta}, \\ & r_A \leq 0, \end{array}$$

$$\text{Dual-B:} \quad \begin{array}{ll} \min & 0 \cdot r_B \\ \text{s.t.} & \boldsymbol{\beta}r_B = \boldsymbol{\theta} + \boldsymbol{\beta}, \\ & r_B \geq 0. \end{array}$$

We want to find the set of $\boldsymbol{\theta}$ such that the optimal values of problems A and B are finite. Then, Dual-A and Dual-B need to have non-empty feasible sets, which implies the following two conditions:

$$\exists r_A \leq 0, \quad \text{s.t.} \quad \boldsymbol{\beta}r_A = \boldsymbol{\theta} - \boldsymbol{\beta}, \quad (10)$$

$$\exists r_B \geq 0, \quad \text{s.t.} \quad \boldsymbol{\beta}r_B = \boldsymbol{\theta} + \boldsymbol{\beta}. \quad (11)$$

For all i with $\beta_i \leq 0$, (10) implies $\theta_i - \beta_i \geq 0$ and (11) implies $\theta_i \leq -\beta_i$. On the other hand, for all j with $\beta_j \geq 0$, (10) and (11) imply $-\beta_j \leq \theta_j \leq \beta_j$. It is not hard to conclude that:

$$|\theta_i| \leq |\beta_i|, \quad \forall i.$$

It follows,

$$\kappa = \sup\{\|\boldsymbol{\theta}\|_* : |\theta_i| \leq |\beta_i|, \forall i\} = \|\boldsymbol{\beta}\|_*.$$

■

Due to Theorem 2.1, (7) could be formulated as the following optimization problem:

$$\inf_{\boldsymbol{\beta} \in \mathcal{B}} \epsilon \|\boldsymbol{\beta}\|_* + \frac{1}{N} \sum_{i=1}^N |\mathbf{z}'_i \boldsymbol{\beta}|. \quad (12)$$

Remark 2.1 (12) incorporates a class of models whose specific form depends on the norm space we choose, which could be application-dependent and practically useful. For example, when the coordinates of \mathbf{z} differ from each other substantially, a properly chosen, positive definite weight matrix \mathbf{M} could scale correspondingly different coordinates of \mathbf{z} by using the \mathbf{M} -weighted norm:

$$\|\mathbf{z}\|_{\mathbf{M}} = \sqrt{\mathbf{z}' \mathbf{M} \mathbf{z}}.$$

By solving the optimality conditions corresponding to (4), it can be shown that the dual norm in this case is just:

$$\|\boldsymbol{\theta}\|_* = \sqrt{\boldsymbol{\theta}' \mathbf{M}^{-1} \boldsymbol{\theta}}.$$

Remark 2.2 When the Wasserstein metric s is induced by $\|\cdot\|_2$ and the set \mathcal{B} is the intersection of a polyhedron with convex quadratic inequalities, (12) is a convex quadratic problem which can be solved to optimality very efficiently. Specifically, it could be converted to:

$$\begin{aligned} \min_{a, b_1, \dots, b_N, \boldsymbol{\beta}} \quad & a\epsilon + \frac{1}{N} \sum_{i=1}^N b_i \\ \text{s.t.} \quad & \|\boldsymbol{\beta}\|_2^2 \leq a^2, \\ & \mathbf{z}'_i \boldsymbol{\beta} \leq b_i, \quad i = 1, \dots, N, \\ & -\mathbf{z}'_i \boldsymbol{\beta} \leq b_i, \quad i = 1, \dots, N, \\ & \boldsymbol{\beta}' \mathbf{e}_m = 1, \\ & a, b_i \geq 0, \quad i = 1, \dots, N, \\ & \boldsymbol{\beta} \in \mathcal{B}. \end{aligned} \quad (13)$$

When the Wasserstein metric is defined using $\|\cdot\|_1$ and the set \mathcal{B} is a poly-

hedron, (12) is a linear programming problem:

$$\begin{aligned}
\min_{a, b_1, \dots, b_N, \boldsymbol{\beta}} \quad & a\epsilon + \frac{1}{N} \sum_{i=1}^N b_i \\
\text{s.t.} \quad & a \geq \boldsymbol{\beta}' \mathbf{e}_i, \quad i = 1, \dots, m, \\
& a \geq -\boldsymbol{\beta}' \mathbf{e}_i, \quad i = 1, \dots, m, \\
& \mathbf{z}'_i \boldsymbol{\beta} \leq b_i, \quad i = 1, \dots, N, \\
& -\mathbf{z}'_i \boldsymbol{\beta} \leq b_i, \quad i = 1, \dots, N, \\
& \boldsymbol{\beta}' \mathbf{e}_m = 1, \\
& a, b_i \geq 0, \quad i = 1, \dots, N, \\
& \boldsymbol{\beta} \in \mathcal{B}.
\end{aligned} \tag{14}$$

Remark 2.3 The parameter ϵ controls the conservativeness of our formulation, whose selection depends on both the sample size and the confidence that the Wasserstein ball contains the true distribution [see eq. (8) in Esfahani and Kuhn, 2015]. Roughly speaking, when the sample size is large enough, and for a fixed confidence level, ϵ is inversely proportional to $N^{1/m}$.

Remark 2.4 When the Wasserstein metric s is induced by some proper norm, (12) is the same with the regularized LAD [Pollard, 1991, Wang et al., 2006]. However, there exist two essential differences that justify the value and novelty of (12). First of all, in the LAD literature, the regularization term is introduced to prevent overfitting (ℓ_2 -regularizer), or to resolve the issue of ill-conditioned design matrix and recover a sparse coefficient vector (ℓ_1 -regularizer). By contrast, the regularizer in (12) is a control over the amount of ambiguity in the data, whose existence is not decided by the sparsity of the coefficient or the correlation among predictors. More importantly, (12) is theoretically rooted and derived from DRO, of which the regularizer is an indispensable ingredient that reveals the reliability of the contaminated samples. Second, the regularization coefficient in (12) is the radius of the Wasserstein ball, which offers an intuitive interpretation and provides guidance on how to set it. This connection is not present in the regularized LAD literature, which starts from the regularized problem rather than obtaining it as an outcome of a more fundamental DRO formulation.

3 Performance Guarantees

In this section we will provide two types of performance guarantees for the solution to (12), one of which is concerned with its performance on new, future data (given in Section 3.1) and applies to any norm induced Wasserstein formulation. The other one that bounds the discrepancy between the estimated and true regression planes, given in Section 3.2, only holds when the Wasserstein metric is defined on the ℓ_1 -norm space.

3.1 Out-of-Sample Performance

In this subsection we investigate generalization characteristics of the solution to (12), which involves measuring the error generated by our estimator on a new random sample \mathbf{z} . We would like to obtain estimates that not only explain the observed samples well, but, more importantly, possess strong generalization abilities. The derivation is mainly based on Rademacher complexity [see Bartlett and Mendelson, 2002], which is a measurement of the complexity of a class of functions. Several mild assumptions are needed in this section.

Assumption A *The norm of the uncertainty parameter \mathbf{z} is bounded above almost surely, i.e., $\|\mathbf{z}\| \leq R$.*

Note that this assumption makes \mathcal{Z} a subset of \mathbb{R}^m , and thus (9) holds with strict inequality, which renders our formulation (12) a reformulation of the original Wasserstein DRO problem (7).

Assumption B *The dual norm of β is bounded above within the feasible region, namely,*

$$\sup_{\beta \in \mathcal{B}} \|\beta\|_* = \bar{B}.$$

We would like to bound the expected loss under these two assumptions. We first bound the Rademacher complexity.

Lemma 3.1 *For every feasible β , it follows*

$$|\mathbf{z}'\beta| \leq \bar{B}R, \quad \text{almost surely.}$$

Lemma 3.1 can be easily proved using (5). Now consider the class of functions:

$$\mathcal{H} = \{\mathbf{z} \mapsto h_\beta(\mathbf{z}) : h_\beta(\mathbf{z}) = |\mathbf{z}'\beta|, \beta \in \mathcal{B}\}.$$

We next show a result about the empirical Rademacher complexity of \mathcal{H} , denoted by $\mathcal{R}_N(\mathcal{H})$, based on the result in Lemma 3.1. The result is similar to Lemma 3 in Bertsimas et al. [2015].

Lemma 3.2

$$\mathcal{R}_N(\mathcal{H}) \leq \frac{2\bar{B}R}{\sqrt{N}}.$$

Proof: Suppose that $\sigma_1, \dots, \sigma_N$ are i.i.d. uniform random variables on $\{1, -1\}$.

Then, by the definition of the Rademacher complexity and Lemma 3.1,

$$\begin{aligned}
\mathcal{R}_N(\mathcal{H}) &= \mathbb{E} \left[\sup_{h \in \mathcal{H}} \frac{2}{N} \left| \sum_{i=1}^N \sigma_i h_{\beta}(\mathbf{z}_i) \right| \middle| \mathbf{z}_1, \dots, \mathbf{z}_N \right] \\
&\leq \frac{2\bar{B}R}{N} \mathbb{E} \left[\left| \sum_{i=1}^N \sigma_i \right| \right] \\
&\leq \frac{2\bar{B}R}{N} \mathbb{E} \left[\sqrt{\sum_{i=1}^N \sigma_i^2} \right] \\
&= \frac{2\bar{B}R}{\sqrt{N}}.
\end{aligned}$$

■

Let $\hat{\beta}$ be an optimal solution to (12), obtained using the samples \mathbf{z}_i , $i = 1, \dots, N$. Suppose we draw a new i.i.d. sample $\mathbf{z} = (\mathbf{x}, y)$. In Theorem 3.3 we establish bounds on the error $|\mathbf{z}'\hat{\beta}|$.

Theorem 3.3 *Under Assumptions A and B, for any $0 < \delta < 1$, with probability at least $1 - \delta$ with respect to the sampling,*

$$\mathbb{E}[|\mathbf{z}'\hat{\beta}|] \leq \frac{1}{N} \sum_{i=1}^N |\mathbf{z}'_i \hat{\beta}| + \frac{2\bar{B}R}{\sqrt{N}} + \bar{B}R \sqrt{\frac{8 \log(2/\delta)}{N}}, \quad (15)$$

and for any $\zeta > \frac{2\bar{B}R}{\sqrt{N}} + \bar{B}R \sqrt{\frac{8 \log(2/\delta)}{N}}$,

$$\mathbb{P} \left(|\mathbf{z}'\hat{\beta}| \geq \frac{1}{N} \sum_{i=1}^N |\mathbf{z}'_i \hat{\beta}| + \zeta \right) \leq \frac{\frac{1}{N} \sum_{i=1}^N |\mathbf{z}'_i \hat{\beta}| + \frac{2\bar{B}R}{\sqrt{N}} + \bar{B}R \sqrt{\frac{8 \log(2/\delta)}{N}}}{\frac{1}{N} \sum_{i=1}^N |\mathbf{z}'_i \hat{\beta}| + \zeta}. \quad (16)$$

Proof: We use Theorem 8 in Bartlett and Mendelson [2002], setting the following correspondences with the notation used there: $\mathcal{L}(\mathbf{x}, y) = \phi(\mathbf{x}, y) = |\mathbf{z}'\beta|$, where $\mathbf{z} = (\mathbf{x}, y)$. This yields the bound (15) on the expected loss. For Eq. (16), we apply Markov's inequality to obtain:

$$\begin{aligned}
\mathbb{P} \left(|\mathbf{z}'\hat{\beta}| \geq \frac{1}{N} \sum_{i=1}^N |\mathbf{z}'_i \hat{\beta}| + \zeta \right) &\leq \frac{\mathbb{E}[|\mathbf{z}'\hat{\beta}|]}{\frac{1}{N} \sum_{i=1}^N |\mathbf{z}'_i \hat{\beta}| + \zeta} \\
&\leq \frac{\frac{1}{N} \sum_{i=1}^N |\mathbf{z}'_i \hat{\beta}| + \frac{2\bar{B}R}{\sqrt{N}} + \bar{B}R \sqrt{\frac{8 \log(2/\delta)}{N}}}{\frac{1}{N} \sum_{i=1}^N |\mathbf{z}'_i \hat{\beta}| + \zeta}.
\end{aligned}$$

■

Remark 3.1 There are two probability measures in the statement of Theorem 3.3. One is related to the new data \mathbf{z} , while the other is related to the samples $\mathbf{z}_1, \dots, \mathbf{z}_N$. The expectation in (15) (and the probability in (16)) is taken w.r.t the new data \mathbf{z} . For a fixed set of samples, (15) (and (16)) holds with probability at least $1 - \delta$ w.r.t. the measure of samples. Theorem 3.3 essentially says that given typical samples, the expected loss on new data using our Wasserstein DRO estimator could be bounded above by the average sample loss plus extra terms that are proportional to $1/\sqrt{N}$. Since a term of (12) minimizes the sample average loss, it is ensured that our estimator achieves good performance on new, future data.

Remark 3.2 Note that the upper bounds in (15) and (16) do not depend on the dimension of \mathbf{z} . This dimensionality-free characteristic implies direct applicability of our Wasserstein approach to high-dimensional settings and is particularly useful in many real applications where, potentially, hundreds of features may be present.

Next we will show two corollaries that provide a guidance on how many samples are needed to achieve satisfactory out-of-sample performance.

Corollary 3.4 *Suppose $\hat{\beta}$ is the optimal solution to (12). For a fixed confidence level δ and some threshold parameter $\tau \geq 0$, to guarantee that the percentage difference between the expected absolute loss on new data and the sample average loss is less than τ , that is,*

$$\frac{\mathbb{E}[|\mathbf{z}'\hat{\beta}|] - \frac{1}{N} \sum_{i=1}^N |\mathbf{z}'_i\hat{\beta}|}{BR} \leq \tau,$$

the sample size N must satisfy

$$N \geq \left[\frac{2(1 + \sqrt{2 \log(2/\delta)})}{\tau} \right]^2. \quad (17)$$

Proof: The percentage difference requirement can be translated into:

$$\frac{2}{\sqrt{N}} + \sqrt{\frac{8 \log(2/\delta)}{N}} \leq \tau,$$

from which (17) can be easily derived. ■

Corollary 3.5 *Suppose $\hat{\beta}$ is the optimal solution to (12). For a fixed confidence level δ , some $\tau \in (0, 1)$ and $\gamma \geq 0$, to guarantee that*

$$\mathbb{P}\left(\frac{|\mathbf{z}'\hat{\beta}| - \frac{1}{N} \sum_{i=1}^N |\mathbf{z}'_i\hat{\beta}|}{BR} \geq \gamma\right) \leq \tau,$$

the sample size N must satisfy

$$N \geq \left[\frac{2(1 + \sqrt{2 \log(2/\delta)})}{\tau \cdot \gamma + \tau - 1} \right]^2, \quad (18)$$

provided that $\tau \cdot \gamma + \tau - 1 > 0$.

Proof: Based on Theorem 3.3, we just need the following inequality to hold:

$$\frac{\frac{1}{N} \sum_{i=1}^N |\mathbf{z}'_i \hat{\boldsymbol{\beta}}| + \frac{2\bar{B}R}{\sqrt{N}} + \bar{B}R \sqrt{\frac{8 \log(2/\delta)}{N}}}{\frac{1}{N} \sum_{i=1}^N |\mathbf{z}'_i \hat{\boldsymbol{\beta}}| + \gamma \bar{B}R} \leq \tau,$$

which is equivalent to:

$$\frac{\gamma \bar{B}R - \frac{2\bar{B}R}{\sqrt{N}} - \bar{B}R \sqrt{\frac{8 \log(2/\delta)}{N}}}{\frac{1}{N} \sum_{i=1}^N |\mathbf{z}'_i \hat{\boldsymbol{\beta}}| + \gamma \bar{B}R} \geq 1 - \tau. \quad (19)$$

We cannot obtain a lower bound for N by directly solving (19) since N appears in a summation operator. A proper relaxation to (19) is:

$$\frac{\gamma - \frac{2}{\sqrt{N}} - \sqrt{\frac{8 \log(2/\delta)}{N}}}{1 + \gamma} \geq 1 - \tau, \quad (20)$$

due to the fact that $\frac{1}{N} \sum_{i=1}^N |\mathbf{z}'_i \hat{\boldsymbol{\beta}}| \leq \bar{B}R$. By solving (20), we obtain (18). ■

Remark 3.3 The sample size is inversely proportional to both δ and τ in (17) and (18), which is reasonable since the more confident we want to be, the more samples we need. Moreover, the smaller τ is, the stricter a requirement we impose on the performance, and thus more samples are needed.

3.2 Discrepancy between Estimated and True Regression Planes

In this section we seek to bound the difference between the estimated and true regression coefficients in the special case where the Wasserstein metric is induced by the ℓ_1 -norm space. Throughout the section we will use $\hat{\boldsymbol{\beta}}$ to denote the estimated regression coefficients, obtained as an optimal solution to (22), and $\boldsymbol{\beta}^*$ for the true (unknown) regression coefficients. The bound we will derive turns out to be related to the Gaussian width of the unit ball in $\|\cdot\|_\infty$, the sub-Gaussian norm of the uncertainty parameter \mathbf{z} , as well as the geometric structure of the true regression coefficients. Some preliminary definitions that are used in later development are presented below.

Definition 3 (Sub-Gaussian random variable) *A random variable z is sub-Gaussian if the ψ_2 -norm defined below is finite, i.e.,*

$$\|z\|_{\psi_2} \triangleq \sup_{q \geq 1} \frac{\mathbb{E}|z|^q}{\sqrt{q}} < +\infty.$$

An equivalent property for sub-Gaussian random variables is that their tail distribution decays as fast as a Gaussian, namely,

$$\mathbb{P}(|z| \geq t) \leq 2 \exp\{-t^2/C^2\}, \quad \forall t \geq 0,$$

for some constant C .

A random vector $\mathbf{z} \in \mathbb{R}^m$ is sub-Gaussian if $\mathbf{z}'\mathbf{u}$ is sub-Gaussian for any $\mathbf{u} \in \mathbb{R}^m$. The ψ_2 -norm of a vector \mathbf{z} is defined as:

$$\|\mathbf{z}\|_{\psi_2} \triangleq \sup_{\mathbf{u} \in \mathbb{S}^m} \|\mathbf{z}'\mathbf{u}\|_{\psi_2},$$

where \mathbb{S}^m denotes the unit sphere in the m -dimensional Euclidean space. For the properties of sub-Gaussian random variables/vectors, please refer to the book by Vershynin [2017].

Definition 4 (Gaussian width) For any set $\mathcal{A} \subseteq \mathbb{R}^m$, its Gaussian width is defined as:

$$w(\mathcal{A}) \triangleq \mathbb{E} \left[\sup_{\mathbf{u} \in \mathcal{A}} \mathbf{u}'\mathbf{g} \right], \quad (21)$$

where $\mathbf{g} \sim \mathcal{N}(\mathbf{0}, \mathbf{I})$ is an m -dimensional standard Gaussian random vector.

Now let us consider problem (12) when the Wasserstein metric is induced by $\|\cdot\|_1$. Based on constrained optimization theory [Bertsekas, 1999], it is equivalent to:

$$\begin{aligned} \min \quad & \|\boldsymbol{\beta}\|_{\infty} \\ \text{s.t.} \quad & \|\boldsymbol{\beta}'\mathbf{Z}\|_1 \leq \gamma_N, \\ & \boldsymbol{\beta} \in \mathcal{B}, \end{aligned} \quad (22)$$

where $\mathbf{Z} = [\mathbf{z}_1 \cdots \mathbf{z}_N]$ is the matrix with columns $\mathbf{z}_1, \dots, \mathbf{z}_N$, and γ_N is some exogenous parameter related to ϵ . (22) is similar to (11) in Chen and Banerjee [2016], with the difference lying in that we impose a constraint on the error instead of the gradient. On the other hand, due to their similarity, we will follow line of development in Chen and Banerjee [2016]. Still, our analysis is self-contained and the bound we obtain is in a different form, which provides meaningful insights into our specific problem. More assumptions are needed to bound the discrepancy between the estimated and true regression coefficients.

Assumption C The ℓ_2 norm of $\boldsymbol{\beta}$ is bounded above within the feasible region, namely,

$$\sup_{\boldsymbol{\beta} \in \mathcal{B}} \|\boldsymbol{\beta}\|_2 = \bar{B}_2.$$

Assumption D (Restricted Eigenvalue Condition) For some set $\mathcal{A}(\boldsymbol{\beta}^*) = \text{cone}\{\mathbf{v} \mid \|\boldsymbol{\beta}^* + \mathbf{v}\|_{\infty} \leq \|\boldsymbol{\beta}^*\|_{\infty}\} \cap \mathbb{S}^m$ and some positive scalar $\underline{\alpha}$,

$$\inf_{\mathbf{v} \in \mathcal{A}(\boldsymbol{\beta}^*)} \mathbf{v}'\mathbf{Z}\mathbf{Z}'\mathbf{v} \geq \underline{\alpha}.$$

Assumption E The true coefficient β^* is a feasible solution of the formulation (22), i.e.,

$$\|\mathbf{Z}'\beta^*\|_1 \leq \gamma_N, \quad \beta^* \in \mathcal{B}.$$

Assumption F \mathbf{z} is a centered sub-Gaussian random vector, i.e., it has zero mean and satisfies the following condition:

$$\|\mathbf{z}\|_{\psi_2} = \sup_{\mathbf{u} \in \mathbb{S}^m} \|\mathbf{z}'\mathbf{u}\|_{\psi_2} \leq \mu.$$

Assumption G The covariance matrix of \mathbf{z} has bounded positive eigenvalues. Set $\Gamma = \mathbb{E}[\mathbf{z}\mathbf{z}']$; then,

$$0 < \lambda_{\min} \triangleq \lambda_{\min}(\Gamma) \leq \lambda_{\max}(\Gamma) \triangleq \lambda_{\max} < \infty.$$

Our first result, which is similar to Lemma 2 in Chen and Banerjee [2016], bounds the ℓ_2 norm of the estimation bias in terms of a quantity that is related to the geometric structure of the true coefficients.

Theorem 3.6 Suppose the true regression coefficient vector is β^* and the solution to (22) is $\hat{\beta}$. For the set $\mathcal{A}(\beta^*) = \text{cone}\{\mathbf{v} \mid \|\beta^* + \mathbf{v}\|_\infty \leq \|\beta^*\|_\infty\} \cap \mathbb{S}^m$, under Assumptions A, D, and E, we have:

$$\|\hat{\beta} - \beta^*\|_2 \leq \frac{2R\gamma_N}{\underline{\alpha}} \Psi(\beta^*), \quad (23)$$

where $\Psi(\beta^*) = \sup_{\mathbf{v} \in \mathcal{A}(\beta^*)} \|\mathbf{v}\|_\infty$.

Proof: Since both $\hat{\beta}$ and β^* (the latter due to Assumption E) are feasible, we have:

$$\begin{aligned} \|\mathbf{Z}'\hat{\beta}\|_1 &\leq \gamma_N, \\ \|\mathbf{Z}'\beta^*\|_1 &\leq \gamma_N, \end{aligned}$$

from which we derive that $\|\mathbf{Z}'(\hat{\beta} - \beta^*)\|_1 \leq 2\gamma_N$. Since $\hat{\beta}$ is an optimal solution to (22) and β^* a feasible solution, it follows that $\|\hat{\beta}\|_\infty \leq \|\beta^*\|_\infty$. This implies that $\nu = \hat{\beta} - \beta^*$ satisfies the condition $\|\beta^* + \mathbf{v}\|_\infty \leq \|\beta^*\|_\infty$ included in the definition of $\mathcal{A}(\beta^*)$ and, furthermore, $(\hat{\beta} - \beta^*)/\|\hat{\beta} - \beta^*\|_2 \in \mathcal{A}(\beta^*)$. Together with Assumption D, this yields

$$(\hat{\beta} - \beta^*)' \mathbf{Z}\mathbf{Z}'(\hat{\beta} - \beta^*) \geq \underline{\alpha} \|\hat{\beta} - \beta^*\|_2^2. \quad (24)$$

On the other hand, from the Cauchy-Schwarz inequality (5):

$$\begin{aligned} (\hat{\beta} - \beta^*)' \mathbf{Z}\mathbf{Z}'(\hat{\beta} - \beta^*) &\leq \|\mathbf{Z}'(\hat{\beta} - \beta^*)\|_1 \|\mathbf{Z}'(\hat{\beta} - \beta^*)\|_\infty \\ &\leq 2\gamma_N \max_i |\mathbf{z}'_i(\hat{\beta} - \beta^*)| \\ &\leq 2\gamma_N \max_i \|\hat{\beta} - \beta^*\|_\infty \|\mathbf{z}_i\|_1 \\ &\leq 2R\gamma_N \|\hat{\beta} - \beta^*\|_\infty. \end{aligned} \quad (25)$$

Combining (24) and (25), we have:

$$\begin{aligned}\|\hat{\boldsymbol{\beta}} - \boldsymbol{\beta}^*\|_2 &\leq \frac{2R\gamma_N \|\hat{\boldsymbol{\beta}} - \boldsymbol{\beta}^*\|_\infty}{\underline{\alpha} \|\hat{\boldsymbol{\beta}} - \boldsymbol{\beta}^*\|_2} \\ &\leq \frac{2R\gamma_N \Psi(\boldsymbol{\beta}^*)}{\underline{\alpha}},\end{aligned}$$

where the last step follows from the fact that $(\hat{\boldsymbol{\beta}} - \boldsymbol{\beta}^*)/\|\hat{\boldsymbol{\beta}} - \boldsymbol{\beta}^*\|_2 \in \mathcal{A}(\boldsymbol{\beta}^*)$. \blacksquare

We see that in the bound given in (23), $\Psi(\boldsymbol{\beta}^*)$ depends only on the geometric structure of $\boldsymbol{\beta}^*$, whereas both γ_N and $\underline{\alpha}$ are related to the random matrix \mathbf{Z} . We therefore would like to further bound these two random quantities in a probabilistic way. Lemma 3.7 provides guidance on setting an upper bound for $\underline{\alpha}$.

Lemma 3.7 *Consider the set $\mathcal{A}_\Gamma = \{\mathbf{w} \in \mathbb{S}^m | \Gamma^{-1/2}\mathbf{w} \in \text{cone}(\mathcal{A}(\boldsymbol{\beta}^*))\}$, where $\mathcal{A}(\boldsymbol{\beta}^*)$ is defined as in Theorem 3.6, and $\Gamma = \mathbb{E}[\mathbf{z}\mathbf{z}']$. Under Assumptions F and G, when the sample size $N \geq C_1\bar{\mu}^4(w(\mathcal{A}_\Gamma))^2$, where $\bar{\mu} = \mu\sqrt{\frac{1}{\lambda_{\min}}}$, and $w(\mathcal{A}_\Gamma)$ is the Gaussian width of \mathcal{A}_Γ , with probability at least $1 - \exp(-C_2N/\bar{\mu}^4)$, we have*

$$\mathbf{v}'\mathbf{Z}\mathbf{Z}'\mathbf{v} \geq \frac{N}{2}\mathbf{v}'\Gamma\mathbf{v}, \quad \forall \mathbf{v} \in \mathcal{A}(\boldsymbol{\beta}^*),$$

where C_1 and C_2 are positive constants.

All omitted proofs in this section can be found in Appendix A. The following lemma relates $w(\mathcal{A}_\Gamma)$, which appears in the statement of Lemma 3.7, with $w(\mathcal{A}(\boldsymbol{\beta}^*))$.

Lemma 3.8 (Lemma 4 in Chen and Banerjee [2016]) *Let μ_0 be the ψ_2 -norm of a standard Gaussian random vector $\mathbf{g} \in \mathbb{R}^m$, and $\mathcal{A}_\Gamma, \mathcal{A}(\boldsymbol{\beta}^*)$ be defined as in Lemma 3.7. Then, under Assumption G,*

$$w(\mathcal{A}_\Gamma) \leq C_3\mu_0\sqrt{\frac{\lambda_{\max}}{\lambda_{\min}}}\left(w(\mathcal{A}(\boldsymbol{\beta}^*)) + 3\right),$$

for some positive constant C_3 .

Combining Lemmas 3.7 and 3.8, we are able to give a tight upper bound for $\underline{\alpha}$ when the sample size satisfies a certain condition related to $w(\mathcal{A}(\boldsymbol{\beta}^*))$.

Corollary 3.9 *Under Assumptions F and G, and the conditions in Lemmas 3.7 and 3.8, when $N \geq \bar{C}_1\bar{\mu}^4\mu_0^2 \cdot \frac{\lambda_{\max}}{\lambda_{\min}}\left(w(\mathcal{A}(\boldsymbol{\beta}^*)) + 3\right)^2$, with probability at least $1 - \exp(-C_2N/\bar{\mu}^4)$,*

$$\mathbf{v}'\mathbf{Z}\mathbf{Z}'\mathbf{v} \geq \frac{N\lambda_{\min}}{2}, \quad \forall \mathbf{v} \in \mathcal{A}(\boldsymbol{\beta}^*),$$

where \bar{C}_1 and C_2 are positive constants.

Proof: Combining Lemmas 3.7 and 3.8, and using the fact that for any $\mathbf{v} \in \mathcal{A}(\boldsymbol{\beta}^*)$,

$$\frac{N}{2} \mathbf{v}' \boldsymbol{\Gamma} \mathbf{v} \geq \frac{N \lambda_{\min}}{2},$$

we can derive the desired result. ■

Next we would like to derive the smallest possible value of γ_N such that $\boldsymbol{\beta}^*$ is feasible. This is accomplished in Lemma 3.10.

Lemma 3.10 *Under Assumptions C and F, for any feasible $\boldsymbol{\beta}$, with probability at least $1 - C_4 \exp(-\frac{C_5^2(w(\mathcal{B}_u))^2}{4\rho^2})$,*

$$\|\boldsymbol{\beta}' \mathbf{Z}\|_1 \leq C \mu \bar{B}_2 w(\mathcal{B}_u),$$

where \mathcal{B}_u is the unit ball of norm $\|\cdot\|_\infty$, $\rho = \sup_{\mathbf{v} \in \mathcal{B}_u} \|\mathbf{v}\|_2$, and C_4, C_5, C positive constants.

Combining Theorem 3.6, Corollary 3.9 and Lemma 3.10, we have the following main performance guarantee result that bounds the estimation bias of the solution to (22).

Theorem 3.11 *Under Assumptions A, C, D, E, F, G, and the conditions of Theorem 3.6, Corollary 3.9 and Lemma 3.10, when $N \geq \bar{C}_1 \bar{\mu}^4 \mu_0^2 \frac{\lambda_{\max}}{\lambda_{\min}} (w(\mathcal{A}(\boldsymbol{\beta}^*)) + 3)^2$, with probability at least $1 - \exp(-C_2 N / \bar{\mu}^4) - C_4 \exp(-C_5^2(w(\mathcal{B}_u))^2 / (4\rho^2))$,*

$$\|\hat{\boldsymbol{\beta}} - \boldsymbol{\beta}^*\|_2 \leq \frac{\bar{C} R \bar{B}_2 \mu}{N \lambda_{\min}} w(\mathcal{B}_u) \Psi(\boldsymbol{\beta}^*). \quad (26)$$

Remark 3.4 From (26) we see that the bound for the ℓ_2 -norm of the estimation bias depends on the geometric structures of both the true coefficients and the norm space that the Wasserstein metric is defined on. Moreover, the bias is decreased as the sample size increases and the uncertainty embedded in \mathbf{z} is reduced.

4 Simulation Experiments

In this section we will apply formulation (12) to a number of synthetic datasets with the Wasserstein metric induced by $\|\cdot\|_2$ and $\|\cdot\|_1$, respectively. The experimental scenarios are designed according to the computational paper by Wisnowski et al. [2001]. Specifically, we consider interior \mathbf{x} -space outliers, which are observations that are abnormal only in the y direction, but have \mathbf{x} values that are within normal range. The motivation for focusing on y -space outliers comes from the CT radiation problem outlined in the Introduction. Recent studies have shown that about half of the US annual exposure to ionizing radiation comes

from medical imaging, particularly CT. Experts usually focus on CT scans with high absolute radiation dose, which is often due to large patients and/or seeking high resolution images. They tend to overlook smaller and skinnier patients (normal \mathbf{x} values) who receive a radiation dose that is not high in absolute value but may be much higher than medically necessary (aberrant y values). It is exactly these patients who are facing the highest carcinogenic risk and we are interested in developing a procedure to detect such cases. Of course, and while this is our motivating application, the applicability of our work is far broader.

Our approach will be tested in three different scenarios differentiated by the location of outliers:

- Scenario 1: randomly scattered outliers;
- Scenario 2: outliers in a cloud at the centroid of the \mathbf{x} -space;
- Scenario 3: outliers in a cloud that is randomly placed in the interior of the \mathbf{x} -space.

Since the mathematical formulation (12) in Section 2 is derived in a linear regression setting, the datasets in this section are constructed based on a linear regression model. In addition, our approach is able to select the most relevant features through incorporating sparsity constraints. Suppose there are K feature variables; the response y for clean observations is obtained through the following:

$$y = \tilde{\beta}_0 + \tilde{\beta}_1 x_1 + \cdots + \tilde{\beta}_K x_K + \eta,$$

where η is a noise term. The response values for outlying observations are placed at a distance δ_R off the regression plane, that is,

$$y = \tilde{\beta}_0 + \tilde{\beta}_1 x_1 + \cdots + \tilde{\beta}_K x_K + \delta_R.$$

We set $\tilde{\beta}_0 = 0.3$, $\tilde{\beta}_1 = \cdots = \tilde{\beta}_K = 0.5$ throughout this section. η is normally distributed with mean 0 and variance σ_η^2 . For clean observations, all features x_1, \dots, x_K come from a normal distribution with mean 7.5 and standard deviation 4.0. The experiments are conducted in different factor settings, where the factors considered are:

- Percentage of outliers q : 20%, 30%;
- Outlying distance δ_R : $3\sigma_\eta, 4\sigma_\eta, 5\sigma_\eta$;
- The number of regressors K : 6, 30.

We will compare the performance of (12) with the ℓ_1 -regularized LAD and robust regression with three cost functions – Huber [Huber, 1964, 1973], Talwar [Hinich and Talwar, 1975], and Fair [Fair, 1974]. It is worth mentioning that the ℓ_1 -regularized LAD is a special case of (12) where the Wasserstein metric is induced by the infinity norm. The choice of the norm space for the Wasserstein metric hinges on the notion of distance, or the way the outliers are planted,

which in our case suggests the use of the ℓ_2 -induced Wasserstein formulation (13). But it would be interesting to see how the ℓ_1 -induced formulation (14) performs and add it into comparison. We note that when the closeness of two points is defined in terms of $\|\cdot\|_1$ in a multi-response scenario, (14) is expected to outperform any other norm-induced Wasserstein model. The performance metrics we use include:

- $\|\tilde{\beta}^{\text{est}} - \tilde{\beta}\|_1$, where $\tilde{\beta}^{\text{est}}$ is the estimated regression coefficient and $\tilde{\beta}$ is the true coefficient determined by the clean data;
- The *Receiver Operating Characteristic (ROC)* curve which plots the true positive rate against the false positive rate, as well as the related *Area Under Curve (AUC)*.

We run 500 replications and take the average of the performance metrics. The Gurobi solver [Gu et al.] is used to solve (13) and (14), where the radius ϵ is chosen to be inversely proportional to $N^{1/m}$ by a factor decided based on AUC. Before providing the details of the experimental results, we summarize our major findings below.

1. All approaches have better performance when q is lower, δ_R is larger, and K is smaller.
2. Our approach performs better than the regularized LAD and robust regression, especially when the number of features K is large.
3. Our approach handles high-dimensional, noisy data pretty well, and could achieve satisfactory performance with very few samples.

4.1 Randomly Scattered Outliers

In this subsection, we consider Scenario 1 where the outliers are randomly scattered in the interior of the \mathbf{x} -space. The feature variables for outlying observations have the same distribution as that of the clean data, but the response values are placed at a distance δ_R off the regression plane. We will investigate the impact of the training sample size and noise variance on the performance of all approaches. Several sets of N and σ_η will be used in our implementation, see Table 1. The test sample size M is 60% of the training size.

The Wasserstein formulations (13) and (14), as well as robust regression, only generate an estimated regression coefficient. The identification of outliers is based on the residual and estimated standard deviation of the noise. Specifically,

$$\text{Outlier} = \begin{cases} \text{YES}, & \text{if } |\text{residual}| > \text{threshold} \times \hat{\sigma}_\eta, \\ \text{NO}, & \text{otherwise,} \end{cases}$$

where $\hat{\sigma}_\eta$ is the standard deviation of residuals in the entire training set. ROC curves are obtained through adjusting the threshold values.

Table 1: Training sample size and noise variance for randomly scattered outliers.

	Number of regressors K			
	6		30	
Training sample size N	20,	60	60,	180
Noise standard deviation σ_η	0.25,	0.5	0.5,	1

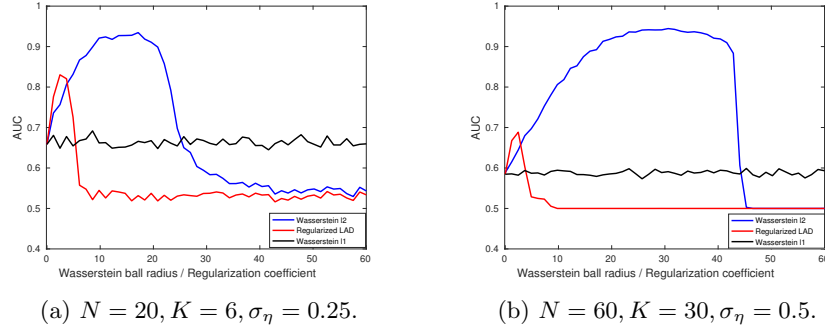


Figure 1: Out-of-sample AUC v.s. Wasserstein ball radius / regularization coefficient for regularized LAD and Wasserstein formulations induced by ℓ_2 and ℓ_1 norms, $q = 30\%$, $\delta_R = 3\sigma_\eta$, and randomly scattered outliers.

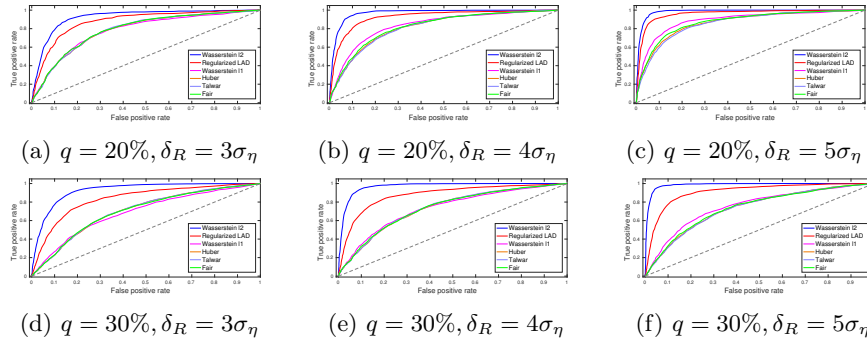


Figure 2: ROC curves for randomly scattered outliers, $N = 20, K = 6, \sigma_\eta = 0.25$.

The Wasserstein radius ϵ is set to be proportional to $1/N^{1/m}$, where the constant factor is chosen to maximize the out-of-sample AUC. The regularization coefficient for LAD is also selected to maximize the AUC. One substantial difference lies in the proportionality of the Wasserstein radius w.r.t. N and m , which implies great savings in computational effort since the parameter tuning procedure in LAD needs to be rerun for every single instance of N and m . In Fig. 1 we plot the out-of-sample AUC as the radius / regularization parameter varies. The Wasserstein ℓ_1 curve (corresponding to (14)) does not contain much useful information, which could be ascribed to the impropriety of using an ℓ_1 notion of distance in our specific case. Regarding the Wasserstein ℓ_2 curve (corresponding to (13)), when ϵ is small, the Wasserstein ball contains the true distribution with low confidence and thus AUC is low. On the other hand, too large ϵ makes our solution overly conservative. Note that the robustness of our approach, indicated by the flatness of the Wasserstein DRO curve, constitutes another advantage, whereas the performance of LAD dramatically deteriorates once the regularizer deviates from the optimum. Moreover, the maximal achievable AUC for Wasserstein DRO is significantly higher than LAD.

The experimental results are properly summarized in the following figures and tables for different combinations of N and σ_η . We note that for all tables, the numbers in parentheses are the results from ℓ_1 -regularized LAD, robust regression with Huber, Talwar, and Fair cost functions, respectively, while the numbers outside parentheses are the results from Wasserstein ℓ_2 (13) and Wasserstein ℓ_1 (14) formulations, respectively. We see that the Wasserstein ℓ_2 formulation consistently outperforms all other approaches, with its ROC curve lying well above others. One could argue that the good performance is due to the way ϵ is chosen, while robust regression does not incorporate such a parameter tuning process. This is indeed a significant factor. LAD seems to be a fairer comparison, yet its performance is remarkably worse than our approach. The Wasserstein ℓ_1 is almost indistinguishable from robust regression due to the unsuitability of an ℓ_1 distance in our specific case. We also want to point out that even if the radius moves a bit away from the optimum, high AUC is still guaranteed for Wasserstein ℓ_2 , as seen from Fig. 1.

More importantly, the superiority of our Wasserstein ℓ_2 formulation could be attributed to its distributional robustness, since we hedge against a family of plausible distributions, including the true distribution with high confidence. By contrast, robust regression adopts an *Iteratively Reweighted Least Squares (IRLS)* procedure which assigns weights to data points based on the residuals from previous iterations. With such an approach, there is a chance of exaggerating the influence of outliers while downplaying the importance of clean observations, especially when the initial residuals are obtained through *Ordinary Least Squares (OLS)*. Talwar’s cost assigns zero weights to observations with residuals above some threshold [see O’Leary, 1990, Fox, 2002], which could very likely discard clean data. Fair’s cost increases at a slower rate than Huber’s cost [see O’Leary, 1990], which might explain its slightly better performance compared to other cost functions.

When we increase σ_η to 0.5 and keep other factors fixed, the AUC in gen-

Table 2: AUC for randomly scattered outliers, $N = 20, K = 6, \sigma_\eta = 0.25$.

Outlying distance	Percentage of outliers	
	20%	30%
3	0.92, 0.78 (0.88, 0.78, 0.78, 0.79)	0.93, 0.69 (0.83, 0.70, 0.70, 0.70)
4	0.97, 0.84 (0.93, 0.82, 0.81, 0.82)	0.97, 0.73 (0.88, 0.73, 0.73, 0.73)
5	0.98, 0.89 (0.96, 0.86, 0.86, 0.87)	0.99, 0.75 (0.91, 0.73, 0.73, 0.74)

Table 3: $\|\tilde{\beta}^{\text{est}} - \tilde{\beta}\|_1$ for randomly scattered outliers, $N = 20, K = 6, \sigma_\eta = 0.25$.

Outlying distance	Percentage of outliers	
	20%	30%
3	0.37, 0.60 (0.46, 0.56, 0.56, 0.57)	0.37, 0.66 (0.47, 0.61, 0.59, 0.62)
4	0.37, 0.63 (0.47, 0.68, 0.68, 0.67)	0.38, 0.75 (0.51, 0.77, 0.76, 0.80)
5	0.37, 0.67 (0.48, 0.76, 0.76, 0.75)	0.38, 0.83 (0.52, 0.96, 0.94, 0.98)

Table 4: AUC for randomly scattered outliers, $N = 20, K = 6, \sigma_\eta = 0.5$.

Outlying distance	Percentage of outliers	
	20%	30%
3	0.97, 0.79 (0.89, 0.79, 0.79, 0.79)	0.97, 0.67 (0.82, 0.67, 0.67, 0.67)
4	0.99, 0.86 (0.93, 0.84, 0.84, 0.85)	0.99, 0.74 (0.89, 0.73, 0.73, 0.73)
5	0.99, 0.89 (0.95, 0.84, 0.84, 0.85)	1.00, 0.78 (0.92, 0.75, 0.75, 0.76)

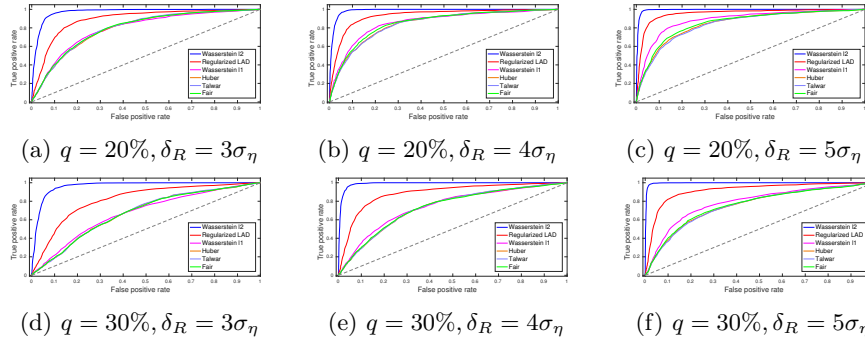


Figure 3: ROC curves for randomly scattered outliers, $N = 20, K = 6, \sigma_\eta = 0.5$.

eral increases due to the fact that the outliers are further away from the true regression plane in the sense of absolute distance, and thus are easier to detect. The AUC increase for Wasserstein ℓ_2 seems to be more significant than robust regression. This is because noisy data tend to distort the fitting plane (as seen from the increase in $\|\tilde{\beta}^{\text{est}} - \tilde{\beta}\|_1$ (Table 5)), especially when the percentage of outliers is high. We note that for $q = 30\%$, $\delta_R = 3$, where outliers are more likely masked, the AUC for robust regression even decreases a bit (Table 4) compared to Table 2. By contrast, the Wasserstein ℓ_2 does not exhibit such a problem due to its distributional robustness. Note also that the increase in $\|\tilde{\beta}^{\text{est}} - \tilde{\beta}\|_1$ for Wasserstein ℓ_2 is less significant than all other approaches. We thus come to the conclusion that the Wasserstein ℓ_2 formulation is less sensitive to noisy data.

Now let us increase the training sample size N . For all approaches, the AUC increases (Table 6) and $\|\tilde{\beta}^{\text{est}} - \tilde{\beta}\|_1$ decreases (Table 7). It is worth mentioning that the Wasserstein ℓ_2 almost achieves perfect AUC for every single case (Table 6), and consistently outperforms both the regularized LAD and robust regression. Even with very few samples, say, $N = 20$, the Wasserstein ℓ_2 still gets an AUC above 90%. The results for $N = 60, K = 6, \sigma_\eta = 0.5$, along with all factor combinations for $K = 30$, convey the same message and can be found in Appendix B.

4.2 Outliers in A Cloud at the Centroid of the \mathbf{x} -Space

In this subsection we consider Scenario 2 where outliers are gathered in a cloud at the centroid of the \mathbf{x} -space. The features for outlying observations are uniformly distributed on the interval $[7.375, 7.625]$ since clean observations have features centered around 7.5. The response values are still at a δ_R distance off the regression plane. Based on our experience in Section 4.1, the sample size and noise variance are set to $N = 20, \sigma_\eta = 0.25$ for $K = 6$; and $N = 60, \sigma_\eta = 0.5$ for $K = 30$. The size of the test dataset is $0.6N$. Note that we use a fairly small sample size relative to the number of features, which is very common in real medical data where there usually exist thousands of features but only hundreds of samples could be obtained (high-dimensional sparsity). The experimental results are presented in Figures 5, 6 and Tables 8, 9, 10, 11.

The poor performance of robust regression is a bit surprising (AUC way below 0.5 for $K = 30, q = 30\%$), especially when compared to the Wasserstein ℓ_2 and regularized LAD. This could be explained by the location of outliers which concentrate at the centroid of clean data. It appears that outliers “compromise” the most essential region of \mathbf{x} -space, while randomly scattered outliers disperse their influence to less important areas. One can draw an analogy to war, where invading the heart of a country generates more devastating consequences. However, the Wasserstein approach seems to achieve very good performance in this scenario, which is reasonable since it is trying to learn the true data-generating mechanism from samples, and centroid outliers do not perturb the distribution of clean samples as much as randomly scattered outliers. Note that for $K = 30$,

Table 5: $\|\tilde{\beta}^{\text{est}} - \tilde{\beta}\|_1$ for randomly scattered outliers, $N = 20, K = 6, \sigma_\eta = 0.5$.

Outlying distance	Percentage of outliers	
	20%	30%
3	0.42, 0.92 (0.61, 1.11, 1.08, 1.12)	0.42, 1.01 (0.66, 1.25, 1.23, 1.29)
4	0.42, 0.97 (0.63, 1.30, 1.29, 1.30)	0.42, 1.09 (0.69, 1.52, 1.49, 1.56)
5	0.42, 1.02 (0.65, 1.60, 1.60, 1.59)	0.42, 1.19 (0.74, 1.85, 1.84, 1.90)

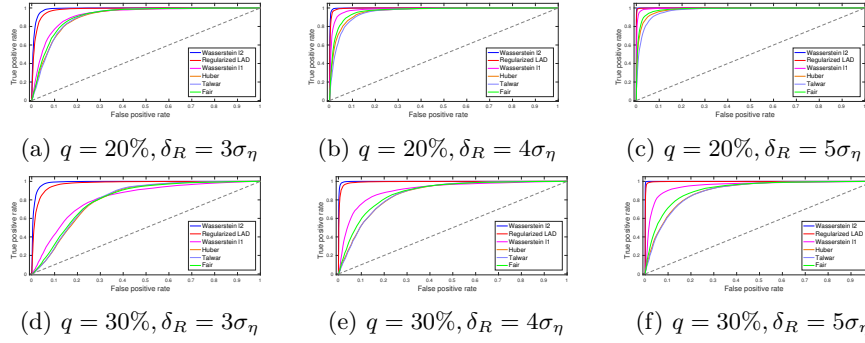


Figure 4: ROC curves for randomly scattered outliers, $N = 60, K = 6, \sigma_\eta = 0.25$.

Table 6: AUC for randomly scattered outliers, $N = 60, K = 6, \sigma_\eta = 0.25$.

Outlying distance	Percentage of outliers	
	20%	30%
3	0.99, 0.92 (0.98, 0.91, 0.91, 0.91)	0.99, 0.82 (0.97, 0.81, 0.81, 0.81)
4	1.00, 0.98 (1.00, 0.96, 0.95, 0.97)	1.00, 0.91 (0.99, 0.86, 0.87, 0.88)
5	1.00, 1.00 (1.00, 0.98, 0.97, 0.99)	1.00, 0.95 (1.00, 0.89, 0.89, 0.91)

Table 7: $\|\tilde{\beta}^{\text{est}} - \tilde{\beta}\|_1$ for randomly scattered outliers, $N = 60, K = 6, \sigma_\eta = 0.25$.

Outlying distance	Percentage of outliers	
	20%	30%
3	0.29, 0.32 (0.38, 0.30, 0.29, 0.30)	0.30, 0.41 (0.39, 0.36, 0.35, 0.37)
4	0.30, 0.32 (0.37, 0.36, 0.36, 0.35)	0.30, 0.43 (0.39, 0.43, 0.43, 0.44)
5	0.29, 0.32 (0.38, 0.43, 0.47, 0.42)	0.30, 0.46 (0.38, 0.54, 0.54, 0.55)

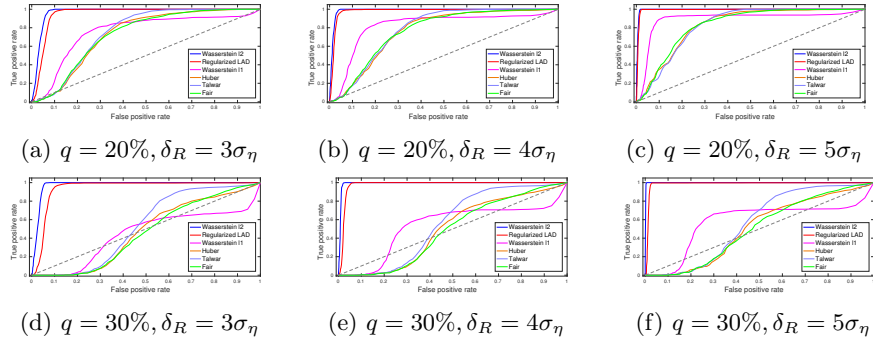


Figure 5: ROC curves for outliers in a centroid cloud, $N = 20, K = 6, \sigma_\eta = 0.25$.

Table 8: AUC for outliers in a centroid cloud, $N = 20, K = 6, \sigma_\eta = 0.25$.

Outlying distance	Percentage of outliers	
	20%	30%
3	0.97, 0.76 (0.95, 0.73, 0.75, 0.73)	0.97, 0.44 (0.94, 0.47, 0.53, 0.46)
4	0.99, 0.82 (0.98, 0.76, 0.78, 0.77)	0.99, 0.53 (0.98, 0.50, 0.56, 0.48)
5	1.00, 0.89 (0.99, 0.83, 0.83, 0.83)	1.00, 0.58 (0.99, 0.51, 0.56, 0.50)

Table 9: $\|\tilde{\beta}^{\text{est}} - \tilde{\beta}\|_1$ for outliers in a centroid cloud, $N = 20, K = 6, \sigma_\eta = 0.25$.

Outlying distance	Percentage of outliers	
	20%	30%
3	0.35, 0.58 (0.46, 0.69, 0.65, 0.69)	0.34, 0.79 (0.45, 1.06, 0.94, 1.03)
4	0.35, 0.61 (0.43, 0.77, 0.73, 0.77)	0.34, 0.85 (0.46, 1.28, 1.15, 1.28)
5	0.35, 0.61 (0.42, 0.85, 0.83, 0.85)	0.34, 0.93 (0.46, 1.53, 1.36, 1.50)

the Wasserstein ℓ_2 formulation achieves perfect AUC with only 60 samples, whereas the regularized LAD, which encompasses a similar parameter tuning procedure, performs remarkably worse, especially when the outlying distance is smaller, in which case aberrant observations are more likely to be masked.

4.3 Outliers in A Cloud Randomly Placed in the Interior \mathbf{x} -Space

We now consider outliers in a cloud that is randomly placed in the interior of the \mathbf{x} -space. The features for outlying observations are uniformly distributed on $(u - 0.125, u + 0.125)$, where u is a uniform random variable on $(7.5 - 3 \times 4, 7.5 + 3 \times 4)$. The response values are at a δ_R distance off the regression plane. The sample size and noise variance are set as in Section 4.2. See Figures 7, 8 and Tables 12, 13, 14, 15 for the experimental results.

The Wasserstein ℓ_2 formulation still outperforms all other approaches, but the difference is not as significant as in Sections 4.1 and 4.2. Outliers in a randomly placed cloud alter the sample distribution significantly and impair the ability to infer the true distribution. On the other hand, the Wasserstein ℓ_2 maintains its AUC level as the number of regressors is raised from 6 to 30, while the regularized LAD, as well as robust regression, gets a significantly lower AUC in a higher dimensional setting (Table 14). We conclude that the Wasserstein approach is able to learn the true data-generating mechanism in high-dimensional settings with very few samples, which makes it a potentially powerful choice in many real applications.

5 Conclusions

We presented a novel outlier detection method based on *Distributionally Robust Optimization (DRO)* in a linear regression framework. The Wasserstein metric was utilized to construct the ambiguity set and a tractable formulation was derived. It is worth noting that the linear law assumption does not limit the applicability of our model. In fact, by pre-processing the data, there indeed exists a roughly linear relationship between the response and the transformed explanatory variables. Our Wasserstein formulation incorporates a class of models whose specific form depends on the norm space that the Wasserstein metric is defined on. We provide out-of-sample performance guarantees for the general formulation, and bound the estimation bias for the ℓ_1 -norm induced Wasserstein formulation. Extensive numerical examples demonstrate the superiority of the Wasserstein formulation compared to the regularized LAD and robust regression. A remarkable advantage of our approach rests in its ability to handle noisy data in a high-dimensional and sparse setting.

Several interesting future research directions are inspired by this work. For example, instead of using a discrete uniform distribution as the center of the Wasserstein ball, one can replace it by a Gaussian distribution, which could be beneficial if there exists evidence of a Gaussian-like data generating mechanism.

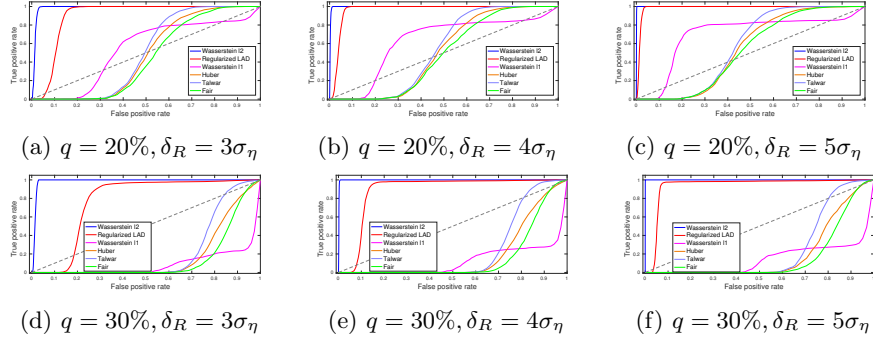


Figure 6: ROC curves for outliers in a centroid cloud, $N = 60, K = 30, \sigma_\eta = 0.5$.

Table 10: AUC for outliers in a centroid cloud, $N = 60, K = 30, \sigma_\eta = 0.5$.

Outlying distance	Percentage of outliers	
	20%	30%
3	0.99, 0.54 (0.89, 0.48, 0.50, 0.45)	0.99, 0.09 (0.77, 0.18, 0.22, 0.15)
4	1.00, 0.62 (0.96, 0.51, 0.54, 0.49)	1.00, 0.13 (0.88, 0.20, 0.25, 0.16)
5	1.00, 0.70 (0.99, 0.55, 0.58, 0.53)	1.00, 0.15 (0.94, 0.20, 0.25, 0.17)

Table 11: $\|\tilde{\beta}^{\text{est}} - \tilde{\beta}\|_1$ for outliers in a centroid cloud, $N = 60, K = 30, \sigma_\eta = 0.5$.

Outlying distance	Percentage of outliers	
	20%	30%
3	0.68, 2.13 (1.26, 3.08, 2.93, 3.20)	0.67, 3.70 (1.49, 5.52, 5.01, 5.69)
4	0.68, 2.34 (1.23, 3.62, 3.43, 3.78)	0.67, 4.38 (1.49, 6.89, 6.01, 6.98)
5	0.68, 2.44 (1.24, 4.23, 3.98, 4.36)	0.67, 4.91 (1.50, 8.99, 8.00, 9.19)

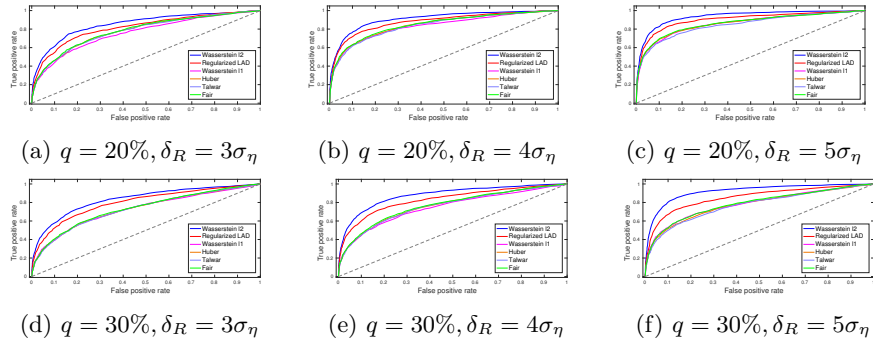


Figure 7: ROC curves for outliers in a randomly placed cloud, $N = 20, K = 6, \sigma_\eta = 0.25$.

Table 12: AUC for outliers in a randomly placed cloud, $N = 20, K = 6, \sigma_\eta = 0.25$.

Outlying distance	Percentage of outliers	
	20%	30%
3	0.85, 0.76 (0.82, 0.78, 0.78, 0.78)	0.83, 0.72 (0.80, 0.73, 0.73, 0.73)
4	0.91, 0.83 (0.88, 0.84, 0.84, 0.85)	0.88, 0.75 (0.83, 0.76, 0.76, 0.77)
5	0.94, 0.86 (0.90, 0.86, 0.85, 0.86)	0.92, 0.78 (0.85, 0.78, 0.77, 0.79)

Table 13: $\|\tilde{\beta}^{\text{est}} - \tilde{\beta}\|_1$ for outliers in a randomly placed cloud, $N = 20, K = 6, \sigma_\eta = 0.25$.

Outlying distance	Percentage of outliers	
	20%	30%
3	0.40, 0.58 (0.46, 0.52, 0.52, 0.52)	0.41, 0.59 (0.47, 0.53, 0.52, 0.54)
4	0.40, 0.61 (0.48, 0.62, 0.63, 0.61)	0.43, 0.67 (0.51, 0.64, 0.63, 0.65)
5	0.41, 0.69 (0.50, 0.73, 0.75, 0.72)	0.43, 0.77 (0.53, 0.81, 0.80, 0.81)

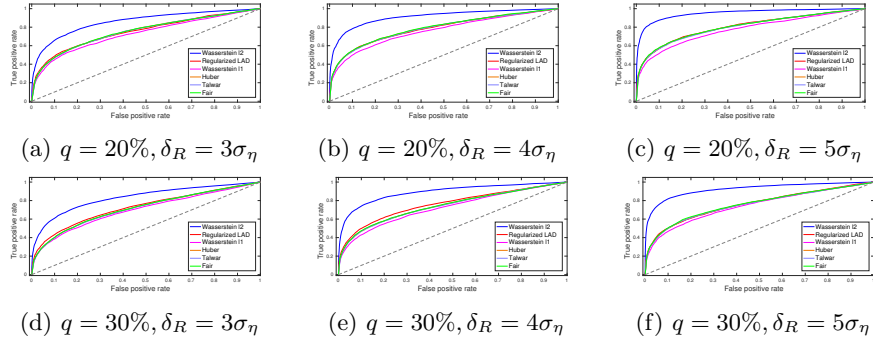


Figure 8: ROC curves for outliers in a randomly placed cloud, $N = 60, K = 30, \sigma_\eta = 0.5$.

Table 14: AUC for outliers in a randomly placed cloud, $N = 60, K = 30, \sigma_\eta = 0.5$.

Outlying distance	Percentage of outliers	
	20%	30%
3	0.86, 0.73 (0.75, 0.75, 0.75, 0.75)	0.83, 0.70 (0.73, 0.71, 0.71, 0.72)
4	0.91, 0.76 (0.78, 0.79, 0.79, 0.79)	0.89, 0.72 (0.76, 0.74, 0.74, 0.74)
5	0.95, 0.77 (0.80, 0.80, 0.80, 0.80)	0.92, 0.74 (0.76, 0.76, 0.76, 0.76)

Generalizations to non-convex uncertainty sets could also be considered. More broadly speaking, the theory we applied in our construction, i.e., DRO, has great potential in developing methodologies for a variety of machine learning problems, e.g., classification. DRO considers the worst possible outcome among a family of distributions learned from samples, which is superior to using just the empirical uniform distribution, as seen in most machine learning techniques. In addition, DRO based on the Wasserstein ambiguity set is usually tractable due to the emerging interest and a plenty of work in the Wasserstein metric and related measure concentration results.

Acknowledgments

Research partially supported by the NSF under grants CCF-1527292, IIS-1237022, and CNS-1645681, by the ARO under grant W911NF-12-1-0390. and by the joint Boston University and Brigham & Women’s Hospital program in Engineering and Radiology. We thank Jenifer Siegelman and Vladimir Valtchinov for useful motivating discussions.

A Omitted Proofs

This section includes the proofs for Lemmas 3.7, 3.8, and 3.10.

A.1 Proof of Lemma 3.7

Proof: Define $\hat{\Gamma} = \frac{1}{N} \sum_{i=1}^N \mathbf{z}_i \mathbf{z}_i'$. Consider the set of functions $\mathcal{F} = \{f_{\mathbf{w}}(\mathbf{z}) = \mathbf{z}'\Gamma^{-1/2}\mathbf{w} | \mathbf{w} \in \mathcal{A}_{\Gamma}\}$. Then, for any $f_{\mathbf{w}} \in \mathcal{F}$,

$$\begin{aligned} \mathbb{E}[f_{\mathbf{w}}^2] &= \mathbb{E}[\mathbf{w}'\Gamma^{-1/2}\mathbf{z}\mathbf{z}'\Gamma^{-1/2}\mathbf{w}] \\ &= \mathbf{w}'\Gamma^{-1/2}\mathbb{E}[\mathbf{z}\mathbf{z}']\Gamma^{-1/2}\mathbf{w} \\ &= \mathbf{w}'\mathbf{w} \\ &= 1, \end{aligned}$$

where we used $\Gamma = \mathbb{E}[\mathbf{z}\mathbf{z}']$ and the fact that $\mathbf{w} \in \mathcal{A}_{\Gamma}$.

For any $f_{\mathbf{w}} \in \mathcal{F}$ we have

$$\begin{aligned}
\|f_{\mathbf{w}}\|_{\psi_2} &= \left\| \mathbf{z}' \mathbf{\Gamma}^{-1/2} \mathbf{w} \right\|_{\psi_2} \\
&= \left\| \mathbf{z}' \mathbf{\Gamma}^{-1/2} \mathbf{w} \right\|_{\psi_2} \frac{\|\mathbf{\Gamma}^{-1/2} \mathbf{w}\|_2}{\|\mathbf{\Gamma}^{-1/2} \mathbf{w}\|_2} \\
&= \left\| \mathbf{z}' \frac{\mathbf{\Gamma}^{-1/2} \mathbf{w}}{\|\mathbf{\Gamma}^{-1/2} \mathbf{w}\|_2} \right\|_{\psi_2} \|\mathbf{\Gamma}^{-1/2} \mathbf{w}\|_2 \\
&\leq \mu \sqrt{\mathbf{w}' \mathbf{\Gamma}^{-1} \mathbf{w}} \\
&\leq \mu \sqrt{\frac{1}{\lambda_{\min}} \|\mathbf{w}\|_2^2} \\
&= \mu \sqrt{\frac{1}{\lambda_{\min}}} = \bar{\mu},
\end{aligned}$$

where the first inequality used Assumption F and the second inequality used Assumption G.

Applying Theorem D from Mendelson et al. [2007], for any $\theta > 0$ and when

$$\tilde{C}_1 \bar{\mu} \gamma_2(\mathcal{F}, \|\cdot\|_{\psi_2}) \leq \theta \sqrt{N},$$

with probability at least $1 - \exp(-\tilde{C}_2 \theta^2 N / \bar{\mu}^4)$ we have

$$\begin{aligned}
\sup_{f_{\mathbf{w}} \in \mathcal{F}} \left| \frac{1}{N} \sum_{i=1}^N f_{\mathbf{w}}^2(\mathbf{z}_i) - \mathbb{E}[f_{\mathbf{w}}^2] \right| &= \sup_{f_{\mathbf{w}} \in \mathcal{F}} \left| \frac{1}{N} \sum_{i=1}^N \mathbf{w}' \mathbf{\Gamma}^{-1/2} \mathbf{z}_i \mathbf{z}_i' \mathbf{\Gamma}^{-1/2} \mathbf{w} - 1 \right| \\
&= \sup_{\mathbf{w} \in \mathcal{A}_{\mathbf{\Gamma}}} \left| \mathbf{w}' \mathbf{\Gamma}^{-1/2} \hat{\mathbf{\Gamma}} \mathbf{\Gamma}^{-1/2} \mathbf{w} - 1 \right| \\
&\leq \theta,
\end{aligned} \tag{27}$$

where \tilde{C}_1 is some positive constant and $\gamma_2(\mathcal{F}, \|\cdot\|_{\psi_2})$ is defined in Mendelson et al. [2007] as a measure of the size of the set \mathcal{F} with respect to the metric $\|\cdot\|_{\psi_2}$. Using $\theta = 1/2$, and properties of $\gamma_2(\mathcal{F}, \|\cdot\|_{\psi_2})$ outlined in Chen and Banerjee [2016], we can set N to satisfy

$$\begin{aligned}
\tilde{C}_1 \bar{\mu} \gamma_2(\mathcal{F}, \|\cdot\|_{\psi_2}) &\leq \tilde{C}_1 \bar{\mu}^2 \gamma_2(\mathcal{A}_{\mathbf{\Gamma}}, \|\cdot\|_2) \\
&\leq \tilde{C}_1 \bar{\mu}^2 C_0 w(\mathcal{A}_{\mathbf{\Gamma}}) \\
&\leq \frac{1}{2} \sqrt{N},
\end{aligned}$$

for some positive constant C_0 , where we used Eq. (44) in Chen and Banerjee [2016]. This implies

$$N \geq C_1 \bar{\mu}^4 (w(\mathcal{A}_{\mathbf{\Gamma}}))^2$$

for some positive constant C_1 . Thus, for such N and with probability at least $1 - \exp(-C_2 N / \bar{\mu}^4)$, for some positive constant C_2 , (27) holds with $\theta = 1/2$.

This implies that for all $\mathbf{w} \in \mathcal{A}_\Gamma$,

$$\left| \mathbf{w}'\Gamma^{-1/2}\hat{\Gamma}\Gamma^{-1/2}\mathbf{w} - 1 \right| \leq \frac{1}{2}$$

or

$$\mathbf{w}'\Gamma^{-1/2}\hat{\Gamma}\Gamma^{-1/2}\mathbf{w} \geq \frac{1}{2} = \frac{1}{2}\mathbf{w}'\Gamma^{-1/2}\Gamma\Gamma^{-1/2}\mathbf{w}.$$

By the definition of \mathcal{A}_Γ , for any $\mathbf{v} \in \mathcal{A}(\beta^*)$,

$$\mathbf{v}'\hat{\Gamma}\mathbf{v} \geq \frac{1}{2}\mathbf{v}'\Gamma\mathbf{v}.$$

Noting that $\hat{\Gamma} = (1/N)\mathbf{Z}\mathbf{Z}'$ yields the desired result. ■

A.2 Proof of Lemma 3.8

We follow the proof of Lemma 4 in Chen and Banerjee [2016], adapted to our setting. We include all key steps for completeness.

Proof: Recall the definition of the Gaussian width $w(\mathcal{A}_\Gamma)$ (cf. (21)):

$$w(\mathcal{A}_\Gamma) = \mathbb{E} \left[\sup_{\mathbf{u} \in \mathcal{A}_\Gamma} \mathbf{u}'\mathbf{g} \right],$$

where $\mathbf{g} \sim \mathcal{N}(\mathbf{0}, \mathbf{I})$. We have:

$$\begin{aligned} \sup_{\mathbf{w} \in \mathcal{A}_\Gamma} \mathbf{w}'\mathbf{g} &= \sup_{\mathbf{w} \in \mathcal{A}_\Gamma} \mathbf{w}'\Gamma^{-1/2}\Gamma^{1/2}\mathbf{g} \\ &= \sup_{\mathbf{w} \in \mathcal{A}_\Gamma} \|\Gamma^{-1/2}\mathbf{w}\|_2 \frac{\mathbf{w}'\Gamma^{-1/2}\Gamma^{1/2}\mathbf{g}}{\|\Gamma^{-1/2}\mathbf{w}\|_2} \\ &\leq \sqrt{\frac{1}{\lambda_{\min}}} \sup_{\mathbf{v} \in \text{cone}(\mathcal{A}(\beta^*)) \cap \mathbb{B}^m} \mathbf{v}'\Gamma^{1/2}\mathbf{g}, \end{aligned}$$

where \mathbb{B}^m is the unit ball in the m -dimensional Euclidean space and the inequality used Assumption G and the fact that $\mathbf{w}'\Gamma^{-1/2}/\|\Gamma^{-1/2}\mathbf{w}\|_2 \in \mathbb{B}^m$ and $\mathbf{w} \in \mathcal{A}_\Gamma$.

Define $\mathcal{T} = \text{cone}(\mathcal{A}(\beta^*)) \cap \mathbb{B}^m$, and consider the stochastic process $\{S_{\mathbf{v}} = \mathbf{v}'\Gamma^{1/2}\mathbf{g}\}_{\mathbf{v} \in \mathcal{T}}$. For any $\mathbf{v}_1, \mathbf{v}_2 \in \mathcal{T}$,

$$\begin{aligned} \|S_{\mathbf{v}_1} - S_{\mathbf{v}_2}\|_{\psi_2} &= \left\| (\mathbf{v}_1 - \mathbf{v}_2)' \Gamma^{1/2} \mathbf{g} \right\|_{\psi_2} \\ &= \|\Gamma^{1/2}(\mathbf{v}_1 - \mathbf{v}_2)\|_2 \left\| \frac{(\mathbf{v}_1 - \mathbf{v}_2)' \Gamma^{1/2} \mathbf{g}}{\|\Gamma^{1/2}(\mathbf{v}_1 - \mathbf{v}_2)\|_2} \right\|_{\psi_2} \\ &\leq \|\Gamma^{1/2}(\mathbf{v}_1 - \mathbf{v}_2)\|_2 \sup_{\mathbf{u} \in \mathbb{S}^m} \|\mathbf{u}'\mathbf{g}\|_{\psi_2} \\ &= \mu_0 \|\Gamma^{1/2}(\mathbf{v}_1 - \mathbf{v}_2)\|_2 \\ &\leq \mu_0 \sqrt{\lambda_{\max}} \|\mathbf{v}_1 - \mathbf{v}_2\|_2, \end{aligned}$$

where the last step used Assumption G.

Then, by the tail behavior of sub-Gaussian random variables (see Hoeffding bound, Thm. 2.6.2 in [Vershynin, 2017]), we have:

$$\mathbb{P}(|S_{\mathbf{v}_1} - S_{\mathbf{v}_2}| \geq \delta) \leq 2 \exp\left(-\frac{C_{01}\delta^2}{\mu_0^2 \lambda_{\max} \|\mathbf{v}_1 - \mathbf{v}_2\|_2^2}\right),$$

for some positive constant C_{01} .

To bound the supremum of $S_{\mathbf{v}}$, we define the metric $s(\mathbf{v}_1, \mathbf{v}_2) = \mu_0 \sqrt{\lambda_{\max}} \|\mathbf{v}_1 - \mathbf{v}_2\|_2$. Then, by Lemma B in Chen and Banerjee [2016],

$$\begin{aligned} \mathbb{E}\left[\sup_{\mathbf{v} \in \mathcal{T}} \mathbf{v}' \mathbf{\Gamma}^{1/2} \mathbf{g}\right] &\leq C_{02} \gamma_2(\mathcal{T}, s) \\ &= C_{02} \mu_0 \sqrt{\lambda_{\max}} \gamma_2(\mathcal{T}, \|\cdot\|_2) \\ &\leq C_3 \mu_0 \sqrt{\lambda_{\max}} w(\mathcal{T}), \end{aligned}$$

for positive constants C_{02}, C_3 , where $\gamma_2(\mathcal{T}, s)$ is the γ_2 -functional we referred to in the proof of Lemma 3.7. Since $\mathcal{T} = \text{cone}(\mathcal{A}(\boldsymbol{\beta}^*)) \cap \mathbb{B}^m \subseteq \text{conv}(\mathcal{A}(\boldsymbol{\beta}^*) \cup \{\mathbf{0}\})$, by Lemma 2 in Maurer et al. [2014],

$$\begin{aligned} w(\mathcal{T}) &\leq w(\text{conv}(\mathcal{A}(\boldsymbol{\beta}^*) \cup \{\mathbf{0}\})) \\ &= w(\mathcal{A}(\boldsymbol{\beta}^*) \cup \{\mathbf{0}\}) \\ &\leq \max\{w(\mathcal{A}(\boldsymbol{\beta}^*)), w(\{\mathbf{0}\})\} + 2\sqrt{\ln 4} \\ &\leq w(\mathcal{A}(\boldsymbol{\beta}^*)) + 3. \end{aligned}$$

Thus,

$$\begin{aligned} w(\mathcal{A}_{\mathbf{\Gamma}}) &= \mathbb{E}\left[\sup_{\mathbf{w} \in \mathcal{A}_{\mathbf{\Gamma}}} \mathbf{w}' \mathbf{g}\right] \\ &\leq \sqrt{\frac{1}{\lambda_{\min}}} \mathbb{E}\left[\sup_{\mathbf{v} \in \mathcal{T}} \mathbf{v}' \mathbf{\Gamma}^{1/2} \mathbf{g}\right] \\ &\leq C_3 \sqrt{\frac{1}{\lambda_{\min}}} \mu_0 \sqrt{\lambda_{\max}} w(\mathcal{T}) \\ &\leq C_3 \mu_0 \sqrt{\frac{\lambda_{\max}}{\lambda_{\min}}} (w(\mathcal{A}(\boldsymbol{\beta}^*)) + 3). \end{aligned}$$

■

A.3 Proof of Lemma 3.10

Proof: By the definition of dual norm (4), we know that:

$$\|\boldsymbol{\beta}' \mathbf{Z}\|_1 = \sup_{\mathbf{v} \in \mathcal{B}_u} \boldsymbol{\beta}' \mathbf{Z} \mathbf{v} = \sup_{\mathbf{v} \in \mathcal{B}_u} \sum_{i=1}^N v_i \boldsymbol{\beta}' \mathbf{z}_i.$$

Since $v_i \boldsymbol{\beta}' \mathbf{z}_i$, $i = 1, \dots, N$ are independent centered sub-Gaussian random variables, and

$$\|v_i \boldsymbol{\beta}' \mathbf{z}_i\|_{\psi_2} \leq \mu \|v_i \boldsymbol{\beta}\|_2,$$

we have that $\sum_{i=1}^N v_i \boldsymbol{\beta}' \mathbf{z}_i$ is also a centered sub-Gaussian random variable with

$$\begin{aligned} \left\| \sum_{i=1}^N v_i \boldsymbol{\beta}' \mathbf{z}_i \right\|_{\psi_2}^2 &\leq C_{03}^2 \sum_{i=1}^N \mu^2 \|v_i \boldsymbol{\beta}\|_2^2 \\ &= C_{03}^2 \mu^2 \|\boldsymbol{\beta}\|_2^2 \|\mathbf{v}\|_2^2, \end{aligned}$$

for a positive constant C_{03} .

Consider the stochastic process $\{S_{\mathbf{v}} = \boldsymbol{\beta}' \mathbf{Z} \mathbf{v}\}_{\mathbf{v} \in \mathcal{B}_u}$. As in the proof of Lemma 3.8,

$$\|S_{\mathbf{v}_1} - S_{\mathbf{v}_2}\|_{\psi_2} \leq C_{03} \mu \|\boldsymbol{\beta}\|_2 \|\mathbf{v}_1 - \mathbf{v}_2\|_2.$$

By the tail behavior of sub-Gaussian random variables [Vershynin, 2017], we know:

$$\mathbb{P}(|S_{\mathbf{v}_1} - S_{\mathbf{v}_2}| \geq \delta) \leq 2 \exp\left(-\frac{C_{04} \delta^2}{\mu^2 \|\boldsymbol{\beta}\|_2^2 \|\mathbf{v}_1 - \mathbf{v}_2\|_2^2}\right).$$

for a positive constant C_{04} .

Define the metric $s(\mathbf{v}_1, \mathbf{v}_2) = \mu \|\boldsymbol{\beta}\|_2 \|\mathbf{v}_1 - \mathbf{v}_2\|_2$. Then, by Lemma B in Chen and Banerjee [2016],

$$\mathbb{P}\left(\sup_{\mathbf{v}_1, \mathbf{v}_2 \in \mathcal{B}_u} |S_{\mathbf{v}_1} - S_{\mathbf{v}_2}| \geq C_{05} (\gamma_2(\mathcal{B}_u, s) + \delta \cdot \text{diam}(\mathcal{B}_u, s))\right) \leq C_4 \exp(-\delta^2).$$

for positive constants C_{05}, C_4 . Also,

$$\begin{aligned} \gamma_2(\mathcal{B}_u, s) &= \mu \|\boldsymbol{\beta}\|_2 \gamma_2(\mathcal{B}_u, \|\cdot\|_2) \leq C_5 \mu \|\boldsymbol{\beta}\|_2 w(\mathcal{B}_u), \\ \text{diam}(\mathcal{B}_u, s) &= \sup_{\mathbf{v}_1, \mathbf{v}_2 \in \mathcal{B}_u} s(\mathbf{v}_1, \mathbf{v}_2) \\ &= \mu \|\boldsymbol{\beta}\|_2 \sup_{\mathbf{v}_1, \mathbf{v}_2 \in \mathcal{B}_u} \|\mathbf{v}_1 - \mathbf{v}_2\|_2 \\ &\leq 2\mu \|\boldsymbol{\beta}\|_2 \sup_{\mathbf{v} \in \mathcal{B}_u} \|\mathbf{v}\|_2 \\ &= 2\mu \|\boldsymbol{\beta}\|_2 \rho. \end{aligned}$$

for positive constants C_5 . Therefore, noting that $\sup_{\mathbf{v}_1, \mathbf{v}_2 \in \mathcal{B}_u} |S_{\mathbf{v}_1} - S_{\mathbf{v}_2}| \geq 2 \sup_{\mathbf{v} \in \mathcal{B}_u} S_{\mathbf{v}}$, we obtain

$$\begin{aligned} &\mathbb{P}\left(\sup_{\mathbf{v} \in \mathcal{B}_u} S_{\mathbf{v}} \geq C_{05} \left(\frac{C_5}{2} \mu \|\boldsymbol{\beta}\|_2 w(\mathcal{B}_u) + \delta \mu \|\boldsymbol{\beta}\|_2 \rho\right)\right) \\ &\leq \mathbb{P}\left(\sup_{\mathbf{v}_1, \mathbf{v}_2 \in \mathcal{B}_u} |S_{\mathbf{v}_1} - S_{\mathbf{v}_2}| \geq C_{05} (\gamma_2(\mathcal{B}_u, s) + \delta \text{diam}(\mathcal{B}_u, s))\right) \\ &\leq C_4 \exp(-\delta^2). \end{aligned}$$

Set $\delta = \frac{C_5 w(\mathcal{B}_u)}{2\rho}$; then with probability at least $1 - C_4 \exp(-\frac{C_5^2(w(\mathcal{B}_u))^2}{4\rho^2})$,

$$\sup_{\mathbf{v} \in \mathcal{B}_u} S_{\mathbf{v}} \leq C\mu\bar{B}_2 w(\mathcal{B}_u).$$

The result follows. ■

B Omitted Figures and Tables

This section includes the omitted figures and tables for randomly scattered outliers.

B.1 Randomly Scattered Outliers, $N = 60, K = 6, \sigma_\eta = 0.5$

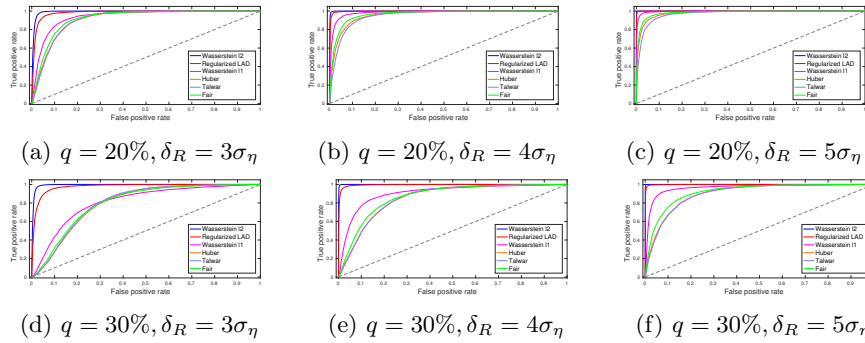


Figure 9: ROC curves for randomly scattered outliers, $N = 60, K = 6, \sigma_\eta = 0.5$.

B.2 Randomly Scattered Outliers, $N = 60, K = 30, \sigma_\eta = 0.5$

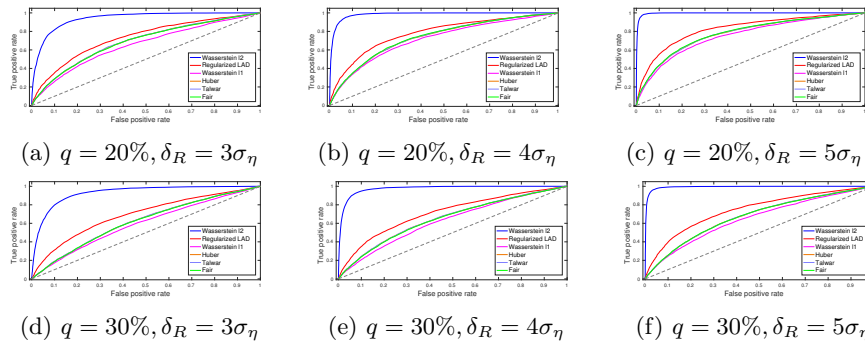


Figure 10: ROC curves for randomly scattered outliers, $N = 60, K = 30, \sigma_\eta = 0.5$.

B.3 Randomly Scattered Outliers, $N = 60, K = 30, \sigma_\eta = 1$

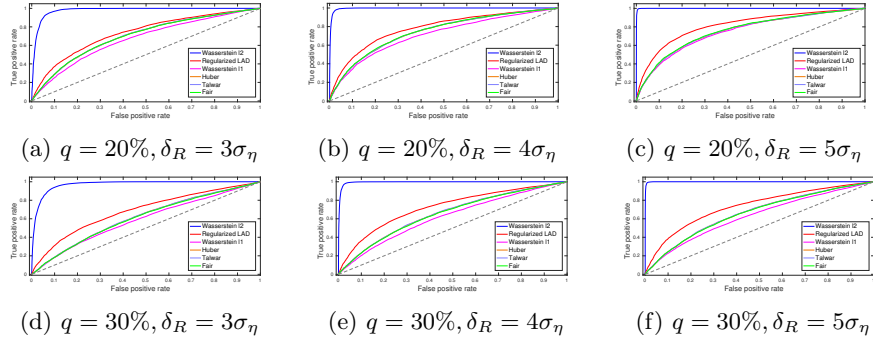


Figure 11: ROC curves for randomly scattered outliers, $N = 60, K = 30, \sigma_\eta = 1$.

B.4 Randomly Scattered Outliers, $N = 180, K = 30, \sigma_\eta = 0.5$

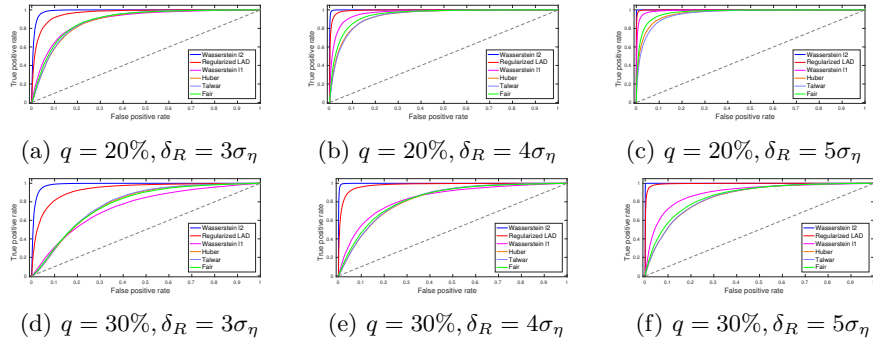


Figure 12: ROC curves for randomly scattered outliers, $N = 180, K = 30, \sigma_\eta = 0.5$.

B.5 Randomly Scattered Outliers, $N = 180, K = 30, \sigma_\eta = 1$

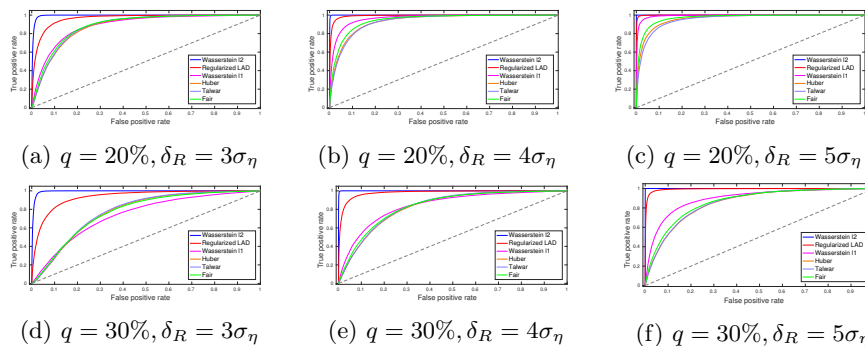


Figure 13: ROC curves for randomly scattered outliers, $N = 180, K = 30, \sigma_\eta = 1$.

References

- Peter L Bartlett and Shahar Mendelson. Rademacher and Gaussian complexities: risk bounds and structural results. *Journal of Machine Learning Research*, 3:463–482, 2002.
- Güzin Bayraksan and David K Love. Data-driven stochastic programming using ϕ -divergences. *Tutorials in Operations Research*, pages 1–19, 2015.
- Dimitri P Bertsekas. *Nonlinear programming*. Athena scientific Belmont, 1999.
- D. Bertsimas, V. Gupta, and I. Ch. Paschalidis. Data-driven estimation in equilibrium using inverse optimization. *Mathematical Programming, Series A*, 153(2):595–633, 2015. doi: dx.doi.org/10.1007/s10107-014-0819-4.
- Chris M Bishop. Training with noise is equivalent to Tikhonov regularization. *Neural computation*, 7(1):108–116, 1995.
- John M Boone, William R Hendee, Michael F McNitt-Gray, and Steven E Seltzer. Radiation exposure from CT scans: how to close our knowledge gaps, monitor and safeguard exposure. *Radiology*, 265(2):544–554, 2012.
- Sheng Chen and Arindam Banerjee. Alternating estimation for structured high-dimensional multi-response models. *arXiv preprint arXiv:1606.08957*, 2016.
- Erick Delage and Yinyu Ye. Distributionally robust optimization under moment uncertainty with application to data-driven problems. *Operations Research*, 58(3):595–612, 2010.
- Laurent El Ghaoui and Hervé Lebret. Robust solutions to least-squares problems with uncertain data. *SIAM Journal on Matrix Analysis and Applications*, 18(4):1035–1064, 1997.

- E Erdoğan and Garud Iyengar. Ambiguous chance constrained problems and robust optimization. *Mathematical Programming*, 107(1-2):37–61, 2006.
- Peyman Mohajerin Esfahani and Daniel Kuhn. Data-driven distributionally robust optimization using the Wasserstein metric: performance guarantees and tractable reformulations. *Available at Optimization Online*, 2015.
- Ray C Fair. On the robust estimation of econometric models. In *Annals of Economic and Social Measurement, Volume 3, number 4*, pages 667–677. NBER, 1974.
- Nicolas Fournier and Arnaud Guillin. On the rate of convergence in Wasserstein distance of the empirical measure. *Probability Theory and Related Fields*, 162(3-4):707–738, 2015.
- John Fox. Robust regression: appendix to an R and S-PLUS companion to applied regression, 2002.
- Rui Gao and Anton J Kleywegt. Distributionally robust stochastic optimization with Wasserstein distance. *arXiv preprint arXiv:1604.02199*, 2016.
- Joel Goh and Melvyn Sim. Distributionally robust optimization and its tractable approximations. *Operations research*, 58(4-part-1):902–917, 2010.
- Zonghao Gu, Edward Rothberg, and Robert Bixby. Gurobi optimizer. <http://www.gurobi.com>.
- Ali S Hadi and Jeffrey S Simonoff. Procedures for the identification of multiple outliers in linear models. *Journal of the American Statistical Association*, 88(424):1264–1272, 1993.
- Melvin J Hinich and Prem P Talwar. A simple method for robust regression. *Journal of the American Statistical Association*, 70(349):113–119, 1975.
- Zhaolin Hu and L Jeff Hong. Kullback-Leibler divergence constrained distributionally robust optimization. *Available at Optimization Online*, 2013.
- Peter J Huber. Robust estimation of a location parameter. *The Annals of Mathematical Statistics*, 35(1):73–101, 1964.
- Peter J Huber. Robust regression: asymptotics, conjectures and Monte Carlo. *The Annals of Statistics*, 1(5):799–821, 1973.
- Ruiwei Jiang and Yongpei Guan. Data-driven chance constrained stochastic program. *Mathematical Programming*, pages 1–37, 2015.
- Leonid Vasilevich Kantorovich and G Sh Rubinstein. On a space of completely additive functions. *Vestnik Leningrad. Univ*, 13(7):52–59, 1958.
- JE Kennedy, MP Quine, et al. The total variation distance between the binomial and Poisson distributions. *The Annals of Probability*, 17(1):396–400, 1989.

- Andreas Maurer, Massimiliano Pontil, and Bernardino Romera-Paredes. An inequality with applications to structured sparsity and multitask dictionary learning. In *COLT*, pages 440–460, 2014.
- Sanjay Mehrotra and He Zhang. Models and algorithms for distributionally robust least squares problems. *Mathematical Programming*, 146(1-2):123–141, 2014.
- Shahar Mendelson, Alain Pajor, and Nicole Tomczak-Jaegermann. Reconstruction and subgaussian operators in asymptotic geometric analysis. *Geometric and Functional Analysis*, 17(4):1248–1282, 2007.
- Dianne P O’Leary. Robust regression computation using iteratively reweighted least squares. *SIAM Journal on Matrix Analysis and Applications*, 11(3):466–480, 1990.
- David Pollard. Asymptotics for least absolute deviation regression estimators. *Econometric Theory*, 7(02):186–199, 1991.
- Ioana Popescu. Robust mean-covariance solutions for stochastic optimization. *Operations Research*, 55(1):98–112, 2007.
- Gilbert L Raff, Kavitha M Chinnaiyan, David A Share, Tauqir Y Goraya, Ella A Kazerooni, Mauro Moscucci, Ralph E Gentry, Aiden Abidov, Advanced Cardiovascular Imaging Consortium Co-Investigators, et al. Radiation dose from cardiac computed tomography before and after implementation of radiation dose–reduction techniques. *Jama*, 301(22):2340–2348, 2009.
- Peter Rousseeuw and Victor Yohai. Robust regression by means of S-estimators. In *Robust and nonlinear time series analysis*, pages 256–272. Springer, 1984.
- Peter J Rousseeuw. Least median of squares regression. *Journal of the American statistical association*, 79(388):871–880, 1984.
- Peter J Rousseeuw. Multivariate estimation with high breakdown point. *Mathematical statistics and applications*, 8:283–297, 1985.
- Peter J Rousseeuw and Annick M Leroy. *Robust regression and outlier detection*. John Wiley & Sons, 2005.
- David M Sebert, Douglas C Montgomery, and Dwayne A Rollier. A clustering algorithm for identifying multiple outliers in linear regression. *Computational statistics & data analysis*, 27(4):461–484, 1998.
- Soroosh Shafieezadeh-Abadeh, Peyman Mohajerin Esfahani, and Daniel Kuhn. Distributionally robust logistic regression. In *Advances in Neural Information Processing Systems*, pages 1576–1584, 2015.
- Alexander Shapiro, Darinka Dentcheva, et al. *Lectures on stochastic programming: modeling and theory*, volume 16. SIAM, 2014.

- Jenifer RQW Siegelman and Dustin A Gress. Radiology stewardship and quality improvement: the process and costs of implementing a CT radiation dose optimization committee in a medium-sized community hospital system. *Journal of the American College of Radiology*, 10(6):416–422, 2013.
- Hailin Sun and Huifu Xu. Convergence analysis for distributionally robust optimization and equilibrium problems. *Mathematics of Operations Research*, 41(2):377–401, 2015.
- William H Swallow and Farid Kianifard. Using robust scale estimates in detecting multiple outliers in linear regression. *Biometrics*, pages 545–556, 1996.
- Roman Vershynin. *High-dimensional probability: An introduction with applications in data science*. Cambridge University Press (to appear), 2017.
- Li Wang, Michael D Gordon, and Ji Zhu. Regularized least absolute deviations regression and an efficient algorithm for parameter tuning. In *Sixth International Conference on Data Mining (ICDM’06)*, pages 690–700. IEEE, 2006.
- Zizhuo Wang, Peter W Glynn, and Yinyu Ye. Likelihood robust optimization for data-driven problems. *Computational Management Science*, 13(2):241–261, 2016.
- Wolfram Wiesemann, Daniel Kuhn, and Melvyn Sim. Distributionally robust convex optimization. *Operations Research*, 62(6):1358–1376, 2014.
- James W Wisnowski, Douglas C Montgomery, and James R Simpson. A comparative analysis of multiple outlier detection procedures in the linear regression model. *Computational Statistics & Data Analysis*, 36(3):351–382, 2001.
- Huan Xu, Constantine Caramanis, and Shie Mannor. Robustness and regularization of support vector machines. *Journal of Machine Learning Research*, 10(Jul):1485–1510, 2009.
- Huan Xu, Constantine Caramanis, and Shie Mannor. Robust regression and lasso. *IEEE Transactions on Information Theory*, 56(7):3561–3574, 2010.
- Victor J Yohai. High breakdown-point and high efficiency robust estimates for regression. *The Annals of Statistics*, pages 642–656, 1987.
- C Zhao and Y Guan. Data-driven risk-averse stochastic optimization with Wasserstein metric. *Available on optimization online*, 2015.
- S. Zymler, D. Kuhn, and B. Rustem. Distributionally robust joint chance constraints with second-order moment information. *Mathematical Programming*, 137(1-2):167–198, 2013.

Table 15: $\|\tilde{\beta}^{\text{est}} - \tilde{\beta}\|_1$ for outliers in a randomly placed cloud, $N = 60, K = 30, \sigma_\eta = 0.5$.

Outlying distance	Percentage of outliers	
	20%	30%
3	0.88, 1.59 (1.24, 1.73, 1.73, 1.73)	0.92, 1.58 (1.58, 1.80, 1.79, 1.81)
4	0.92, 1.77 (1.41, 2.05, 2.07, 2.03)	0.98, 1.90 (1.50, 2.24, 2.23, 2.26)
5	0.95, 2.00 (1.57, 2.57, 2.60, 2.55)	1.05, 2.16 (2.19, 2.78, 2.78, 2.77)

Table 16: AUC for randomly scattered outliers, $N = 60, K = 6, \sigma_\eta = 0.5$.

Outlying distance	Percentage of outliers	
	20%	30%
3	0.99, 0.94 (0.98, 0.91, 0.91, 0.92)	0.99, 0.81 (0.98, 0.80, 0.80, 0.80)
4	1.00, 0.98 (1.00, 0.96, 0.95, 0.96)	1.00, 0.91 (1.00, 0.85, 0.85, 0.87)
5	1.00, 0.99 (1.00, 0.98, 0.97, 0.98)	1.00, 0.96 (1.00, 0.90, 0.90, 0.92)

Table 17: $\|\tilde{\beta}^{\text{est}} - \tilde{\beta}\|_1$ for randomly scattered outliers, $N = 60, K = 6, \sigma_\eta = 0.5$.

Outlying distance	Percentage of outliers	
	20%	30%
3	0.33, 0.54 (0.44, 0.60, 0.59, 0.59)	0.33, 0.69 (0.47, 0.73, 0.71, 0.76)
4	0.33, 0.57 (0.43, 0.72, 0.72, 0.69)	0.33, 0.74 (0.47, 0.94, 0.93, 0.96)
5	0.33, 0.57 (0.43, 0.79, 0.86, 0.78)	0.33, 0.72 (0.46, 1.09, 1.09, 1.08)

Table 18: AUC for randomly scattered outliers, $N = 60, K = 30, \sigma_\eta = 0.5$.

Outlying distance	Percentage of outliers	
	20%	30%
3	0.94, 0.65 (0.73, 0.69, 0.69, 0.69)	0.93, 0.59 (0.69, 0.62, 0.62, 0.62)
4	0.98, 0.72 (0.78, 0.73, 0.74, 0.74)	0.98, 0.62 (0.71, 0.65, 0.65, 0.65)
5	1.00, 0.75 (0.83, 0.77, 0.77, 0.78)	0.99, 0.65 (0.74, 0.67, 0.67, 0.67)

Table 19: $\|\tilde{\beta}^{\text{est}} - \tilde{\beta}\|_1$ for randomly scattered outliers, $N = 60, K = 30, \sigma_\eta = 0.5$.

Outlying distance	Percentage of outliers	
	20%	30%
3	0.80, 1.77 (1.34, 1.99, 1.96, 2.01)	0.84, 1.89 (1.82, 2.16, 2.15, 2.22)
4	0.78, 1.94 (1.52, 2.44, 2.42, 2.46)	0.84, 2.18 (2.20, 2.84, 2.82, 2.90)
5	0.80, 2.19 (1.70, 2.88, 2.86, 2.91)	0.85, 2.53 (2.51, 3.32, 3.30, 3.38)

Table 20: AUC for randomly scattered outliers, $N = 60, K = 30, \sigma_\eta = 1$.

Outlying distance	Percentage of outliers	
	20%	30%
3	0.98, 0.67 (0.73, 0.70, 0.70, 0.70)	0.97, 0.59 (0.69, 0.61, 0.61, 0.61)
4	1.00, 0.71 (0.78, 0.74, 0.74, 0.74)	1.00, 0.62 (0.72, 0.65, 0.65, 0.65)
5	1.00, 0.75 (0.82, 0.75, 0.75, 0.76)	1.00, 0.63 (0.73, 0.66, 0.66, 0.66)

Table 21: $\|\tilde{\beta}^{\text{est}} - \tilde{\beta}\|_1$ for randomly scattered outliers, $N = 60, K = 30, \sigma_\eta = 1$.

Outlying distance	Percentage of outliers	
	20%	30%
3	0.99, 2.90 (2.94, 3.88, 3.85, 3.93)	1.03, 3.13 (3.27, 4.41, 4.39, 4.54)
4	0.99, 3.30 (2.76, 4.99, 4.94, 5.01)	1.03, 3.74 (3.93, 5.62, 5.56, 5.78)
5	0.99, 3.80 (3.16, 5.97, 5.92, 6.02)	1.04, 4.23 (4.58, 6.64, 6.58, 6.76)

Table 22: AUC for randomly scattered outliers, $N = 180, K = 30, \sigma_\eta = 0.5$.

Outlying distance	Percentage of outliers	
	20%	30%
3	0.99, 0.89 (0.97, 0.88, 0.88, 0.89)	0.99, 0.74 (0.93, 0.78, 0.78, 0.77)
4	1.00, 0.97 (0.99, 0.93, 0.93, 0.95)	1.00, 0.84 (0.98, 0.82, 0.83, 0.83)
5	1.00, 0.99 (1.00, 0.96, 0.95, 0.97)	1.00, 0.90 (1.00, 0.85, 0.85, 0.86)

Table 23: $\|\tilde{\beta}^{\text{est}} - \tilde{\beta}\|_1$ for randomly scattered outliers, $N = 180, K = 30, \sigma_\eta = 0.5$.

Outlying distance	Percentage of outliers	
	20%	30%
3	0.52, 0.98 (0.73, 0.99, 0.95, 0.99)	0.54, 1.16 (0.88, 1.08, 1.06, 1.15)
4	0.52, 0.96 (0.73, 1.21, 1.17, 1.15)	0.54, 1.28 (0.82, 1.38, 1.35, 1.45)
5	0.52, 0.95 (0.73, 1.38, 1.38, 1.31)	0.54, 1.36 (0.83, 1.62, 1.59, 1.67)

Table 24: AUC for randomly scattered outliers, $N = 180, K = 30, \sigma_\eta = 1$.

Outlying distance	Percentage of outliers	
	20%	30%
3	0.99, 0.88 (0.96, 0.88, 0.88, 0.89)	0.99, 0.74 (0.93, 0.77, 0.78, 0.77)
4	1.00, 0.97 (0.99, 0.93, 0.93, 0.94)	1.00, 0.84 (0.98, 0.83, 0.83, 0.83)
5	1.00, 0.99 (1.00, 0.96, 0.95, 0.97)	1.00, 0.90 (0.99, 0.85, 0.85, 0.86)

Table 25: $\|\tilde{\beta}^{\text{est}} - \tilde{\beta}\|_1$ for randomly scattered outliers, $N = 180, K = 30, \sigma_\eta = 1$.

Outlying distance	Percentage of outliers	
	20%	30%
3	0.67, 1.60 (1.16, 1.89, 1.82, 1.89)	0.68, 1.89 (1.47, 2.10, 2.06, 2.23)
4	0.67, 1.61 (1.17, 2.34, 2.27, 2.25)	0.69, 2.11 (1.37, 2.72, 2.67, 2.85)
5	0.67, 1.62 (1.17, 2.78, 2.76, 2.63)	0.69, 2.25 (1.40, 3.29, 3.23, 3.42)